New Models for Submarine Channel Deposits on Structurally Complex Slopes: Examples from the Niger Delta System

ABSTRACT

Submarine channel complexes are often described as having a two-phase stratigraphic evolution where an initial phase of migration is followed by aggradation, generating a 'hockey-stick shaped' channel trajectory. However, the role of tectonic forcing in modifying time-integrated sedimentary architectures remains poorly understood. Here, we evaluate how tectonically driven changes in slope modify the evolution—both in terms of morphology and stratigraphic architecture—of submarine channels across a range of spatial scales from the fundamental architectural unit, a channel element, to the scale of a channel complex set, using examples from the Niger Delta system.

From a 3D, time-migrated seismic reflection volume, we use amplitude extractions, frequency decomposition and RGB blending to determine channel stratigraphic architectures. These observations are used systematically to evaluate the development of cross-sectional and planform architectures as the channel systems interact with a range of active and pre-existing structural bathymetry. Our results indicate that while a channel complex's stratigraphic architecture may be captured by a two-phase evolution on unstructured slopes, this model fails on structurally complex slopes. Unstructured slope channel complexes display a repeated arrangement of migration dominating the early stratigraphic record and subsequent aggradation. The late aggradational phase signals a decrease in the rate of growth in channel complex width and the rate of change in sinuosity relative to aggradation throughout the complex's development. However, tectonically driven changes in sinuosity and the relative rates of channel migration and aggradation modify complex development significantly. We identify three end-member styles of channel-structure interaction, determined by the timing of

bathymetry development and its associated style: (1) pre-channel structural bathymetry; (2) coeval positive relief, and (3) coeval negative relief. Where structural relief pre-dates channel inception, a principal adjustment is in the initial channel course with early channel elements being forced around positive relief of the structure, generating long-wavelength bends in the complex's course. Where structure continues to modify slope creating positive and negative bathymetry during complex development, migration and bend development continue with complex width and channel element sinuosity increasing until abandonment. These observations demonstrate that submarine channel architecture and planform are highly sensitive to tectonic perturbation and we use these results to generate graphical models that show predicted architectural evolution of submarine channels on structurally complex slopes in general.

1. INTRODUCTION

Over the past two decades, the increased availability of high-resolution 3D seismic data and its integration with outcrop and numerical modelling studies have substantially improved our understanding of submarine channel architecture and evolution (e.g., Mayall & Stewart, 2000; Abreu et al., 2003; Deptuck et al., 2003, 2007, 2012; Posamentier & Kolla, 2003; Mayall et al., 2006; Kolla et al., 2007; Labourdette & Bez, 2010; McHargue et al., 2011; Sylvester et al., 2011; Janocko et al., 2013; Hansen et al., 2017; Covault et al. 2019). However, the variability and architectural complexity of these systems means that key aspects of their development (e.g., channel incision, aggradation, and lateral migration) remain poorly constrained (Deptuck et al., 2003; Mayall et al., 2006; Sylvester et al., 2011).

Sinuosity development and the style and degree of lateral migration are increasingly recognised as key controls on the stratigraphic architecture of submarine channel complexes (e.g., Mayall et al., 2006; Kolla et al., 2007; Wynn et al., 2007; Sylvester et al., 2011; Janocko et al., 2013; Jobe et al., 2016; Hansen et al., 2017; Covault et al., 2019). Several authors have described submarine channel complexes with a stratigraphic evolution analogous to the 'two-phase' model described in Jobe et al. (2016), which was derived from an analysis of 297 submarine channel sections from across the globe (e.g., Peakall et al., 2000; Deptuck et al., 2007; Hodgson et al., 2011; McHargue et al., 2011). An initial phase of channel element migration is followed by a phase where aggradation dominates, generating a hockey-stick-shaped channel trajectory. A key implication of the 'two-phase' model is that bend formation in submarine channels occurs at a relatively early stage before the development of an apparently stable planform, at which point the flows are in equilibrium with respect to the channel planform (see Peakall et al., 2000). Once this stable equilibrium is reached, changes in complex width should be less significant and a stable planform morphology is maintained (Peakall et al., 2000). Numerous mechanisms have been proposed to explain this evolution including flow properties (Kolla et al., 2007; Jobe et al., 2016), levee growth (Peakall et al., 2000), changes in base level and sediment supply versus accommodation space (Kneller, 2003; McHargue et al. 2011; Sylvester et al. 2011, 2012), and changes in longitudinal profile (Pirmez et al., 2000; Hodgson et al., 2011). Yet, despite the recognition that tectonically driven changes in slope modify channel behaviour, few studies examine how recent and active tectonic deformation may alter this model (e.g. Clark & Cartwright, 2009, 2011; Deptuck et al., 2012; Covault et al., 2020). For instance, underlying structure may increase channel complex sinuosity through *diversion*, where the initial channel course is forced by pre-existing structural bathymetry, and *deflection*, where channel elements successively shift away from bathymetry created by active structure (Clark & Cartwright, 2009, 2011; Kane et al., 2010; Mayall et al., 2010). While both these processes can influence the architectural evolution of submarine channels, a detailed conceptual or predictive model of how this happens, derived from observational datasets, has yet to be comprehensively established.

Here, we address this challenge. We evaluate how tectonically driven changes in slope modify the evolution—both in terms of planform morphology and stratigraphic architecture—of submarine channel systems across a range of spatial scales from channel element to complex set. The documented changes in stratigraphic architecture allow us to analyse how structure has affected both sinuosity development and the relative rates of channel migration and aggradation. In so doing, we assess the tectonic control on the style of bend transformation and the development of architectures associated with sinuous channel systems. Finally, we critically analyse extant models for submarine channel evolution in the context of our data sets and provide new insights into the influence of structure on the architecture of submarine channels across a range of spatial scales and within a well-defined hierarchy.

We use high-resolution, three-dimensional seismic-reflection data from the southern lobe of the Niger Delta to explore channel-structure interactions (Fig. 1). A number of exceptionally well imaged Pleistocene submarine channel deposits were identified in the data covering the spectrum from erosional to constructional channel systems (e.g., Channel complexes 1 to 6; Fig. 2). Here, we focus on two of these channel systems (1 and 5 on Fig. 2) which extend over 120 km downslope and interact with a number of styles of gravity-driven structures, including a relatively undeformed translational domain, a strike-slip transfer zone, and two fold-thrust-belts. Latest Pleistocene - Recent deposition on the slope has been dominated by deposition of draping strata with relatively low-amplitude parallel reflections that taper down-system (c.f. Jobe et al., 2015; Mitchell et al., 2021). Consequently, the older of the systems (channel five) is largely infilled, with only minor present-day geomorphic expression across the outer fold-thrust belt, where hemipelagic deposits are thin. The younger channel one is only partially infilled and has significant (up to 160 m) present-day geomorphic expression along its length (c.f. Mitchell et al., 2021) (Fig.1b). The relative ages of the two systems are stratigraphically clear from a high-amplitude lobe which separates the two systems, infilling the upper part of channel five and underlying channel one (Fig. 2).

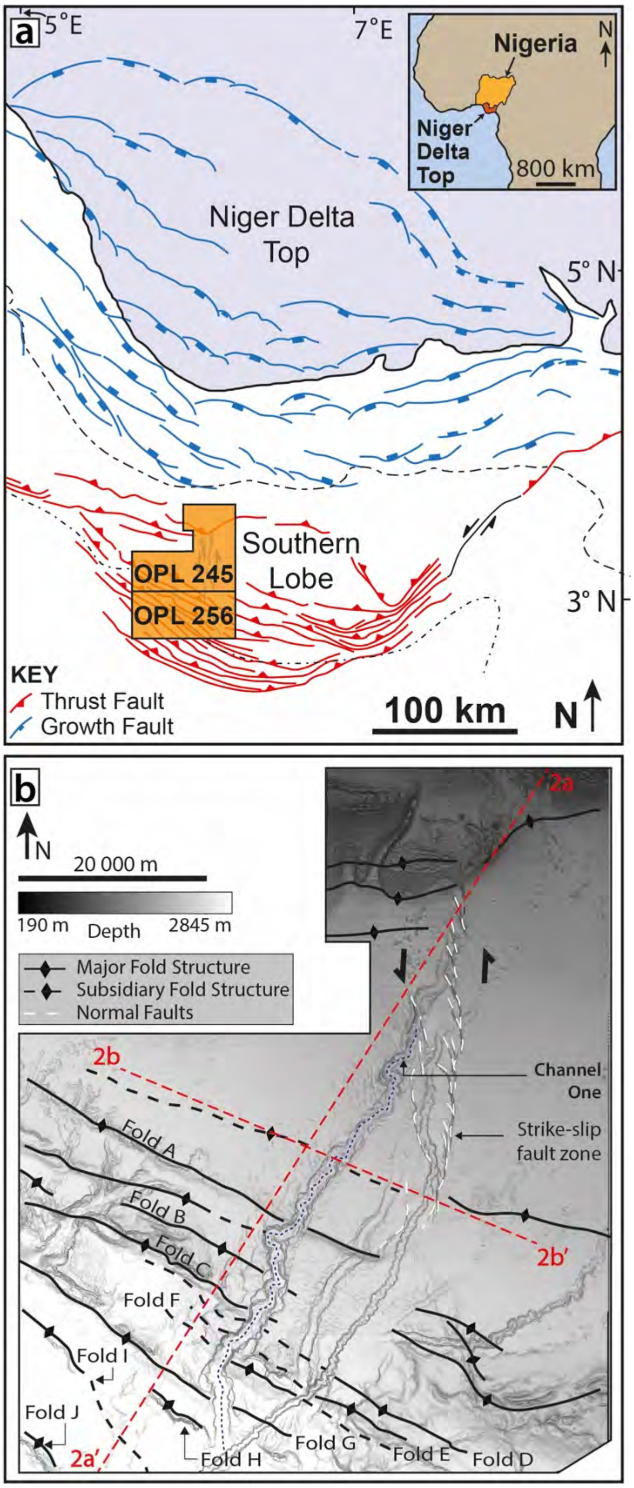

Figure 1. (a) Map showing the location of the study area covering blocks OPL 245 and 256 (highlighted in orange) on the Southern Lobe of the Niger Delta. The location of major structures is also shown (see key). (b) Bathymetry map of the seabed for the study area showing the geomorphic expression of channel one, and the folds that occur at, or near, the seabed (labelled A–J).

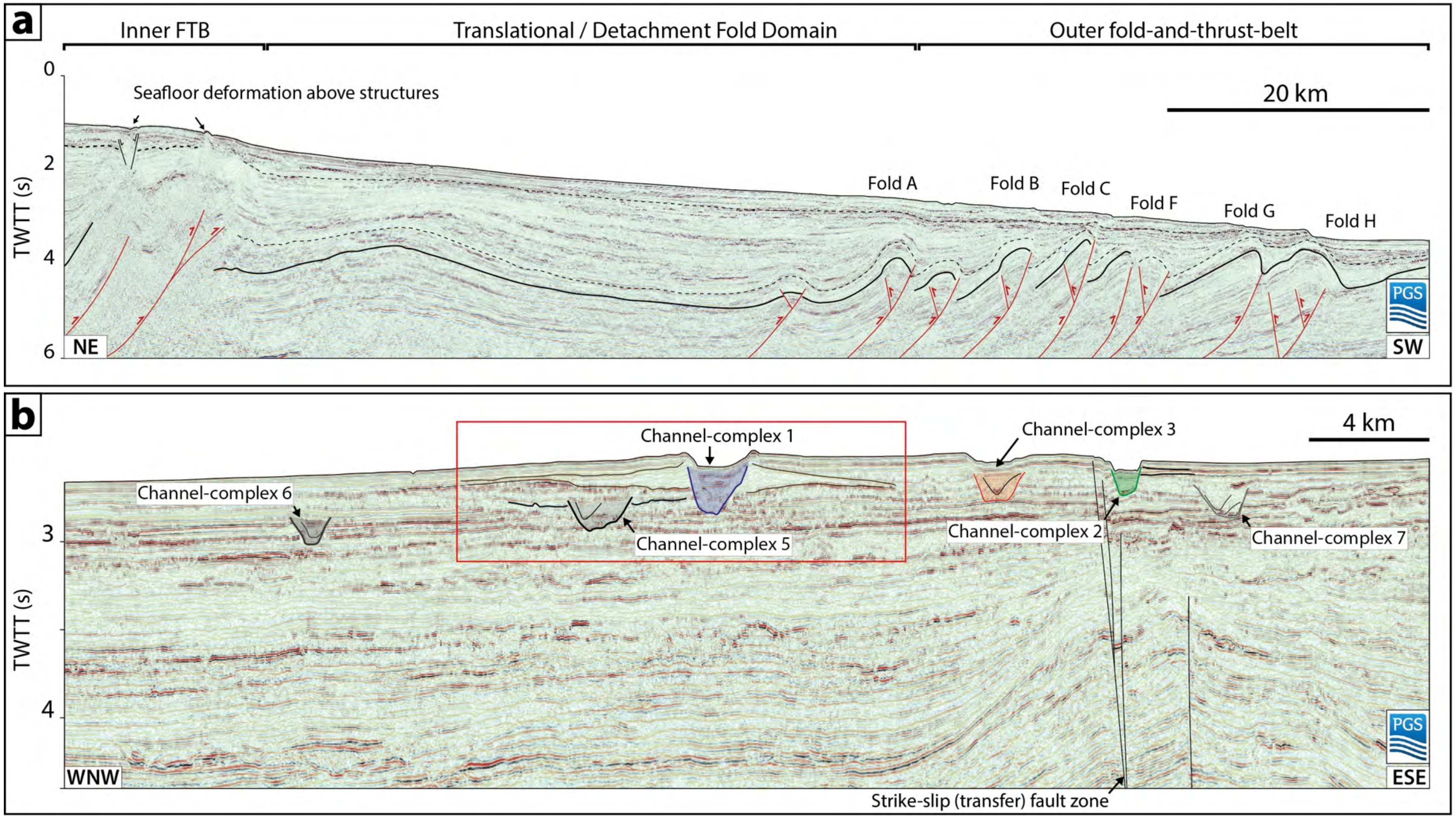

Figure 2. (a) Regional seismic line showing the range of structures and the structural domains which occur within the study area. (b) Seismic section, taken perpendicular to regional dip, showing the submarine channel deposits identified within the dataset. The focus of the study is two Pleistocene submarine channels, one and five (highlighted by red box), which extend across the dataset for over 120 km.

2. TERMINOLOGY

Cross sections taken through submarine channels, either in outcrop or seismic reflection data, often show a complex array of erosional surfaces across multiple scales (Deptuck et al., 2003; Mayall et al., 2006; Sylvester et al., 2011; Deptuck & Sylvester, 2018). This has led to the development of numerous hierarchical classifications that attempt to give spatial and temporal order to sedimentary bodies based on the relationships between their erosional bounding surfaces (e.g., Gardner & Borer, 2000; Gardner et al., 2003; Sprague et al., 2002; 2005; Mayall et al., 2006; Cullis et al., 2018). Here, we follow the hierarchical classification of McHargue et al., (2011) which is appropriate and easy to apply for seismic-based studies. The fundamental architectural unit is defined as the channel element. Each channel element constitutes an erosional bounding surface and the sediments which fill it (Fig. 3). The classification of a channel element has no implication in terms of physical size. Channel elements are distinguished by an abrupt lateral offset of seismic facies and the presence of a reincision surface. Where multiple genetically related elements stack in a consistent pattern, this constitutes a single channel complex: a composite sedimentary body made up of several channel elements (Fig. 3). If two or more complexes are present, they constitute a single complex set (Fig. 3). The use of the terms channel and system are general used to refer to all of the genetically related erosional and depositional components present in a single area, regardless of hierarchy.

Submarine channel systems exist within a spectrum from erosionally confined systems, lacking significant external levees, through systems with varying degrees of erosion and construction, to constructional complexes confined by their external levees alone (Fig. 3) (Broucke et al., 2004; McHargue et al., 2011; Janocko et al., 2013). Here, we use these three broad categories: erosional, erosional-constructional, and constructional—to subdivide the two channel systems based on their mechanism of confinement over a given channel length (Fig. 3).

136
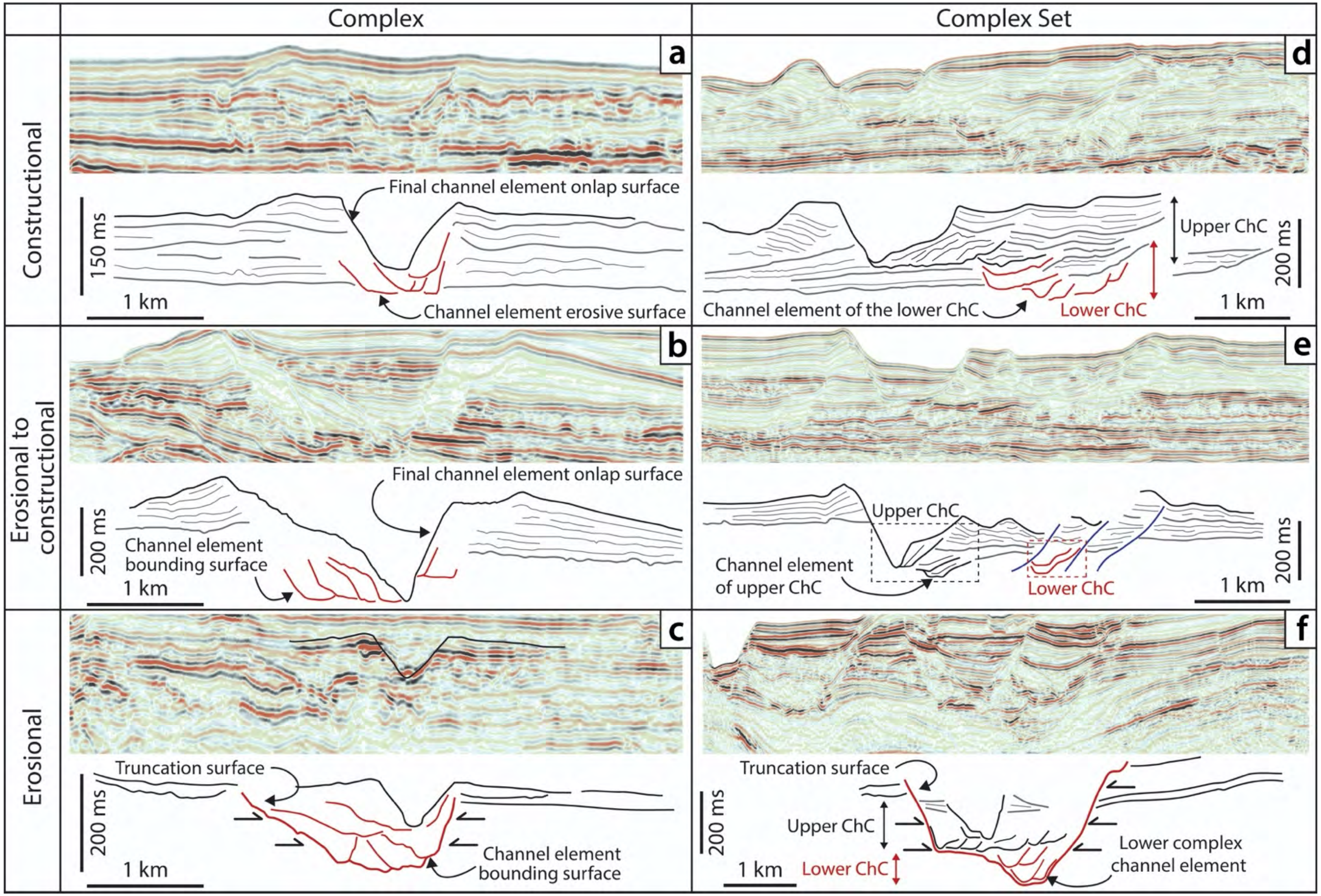
Complex
Complex Set
Constructional
Erosional to constructional
Erosional
a
Final channel element onlap surface
150 ms
1 km
Channel element erosive surface
d
Upper ChC
200 ms
1 km
Channel element of the lower ChC
Lower ChC
b
Final channel element onlap surface
200 ms
Channel element bounding surface
1 km
e
Upper ChC
200 ms
Channel element of upper ChC
Lower ChC
1 km
c
Truncation surface
200 ms
1 km
Channel element bounding surface
f
Truncation surface
200 ms
Upper ChC
1 km
Lower ChC
Lower complex channel element

Figure 3. Seismic sections and line drawings illustrating the basic terminology and classification used in this study. (a) Constructional channel complexes, where a complex is confined by its external levees. (b) Erosional to constructional complexes, where a complexes lower fill is confined by erosional margins, but its upper stratigraphy is confined by external levees. (c) Erosional channel complexes, where a complex lacks external levees. (d) Multiple constructional channel complexes, confined by external levees, amalgamate to form a constructional channel complex set. (e) A system evolves from an erosionally confined lower to a levee-confined system as multiple channel complexes stack and amalgamate. (f) Multiple channel complexes amalgamate within erosional margins to form an erosional channel complex set.

3. GEOLOGICAL SETTING AND STUDY AREA

The Niger Delta, Gulf of Guinea, is one of the largest regressive delta systems in the world with an area of ca.140,000 km^2 and a sedimentary wedge ca. 12 km thick (Damuth, 1994; Kulke, 1995). The stratigraphy is sub-divided into three diachronous units: the Akata, Agbada and Benin Formations (Doust & Omatsola, 1989). In deep water, the deltaic deposits, characteristic of the Agbada Formation, transition into sheet sands, mass transport complexes (MTCs), hemi-pelagic mudstones, and the submarine channel systems on which this study focusses (Krueger & Grant, 2011).

Gravity-driven deformation along regional detachments within the Akata shales has significantly affected the sedimentary wedge, creating an upslope extensional domain that is compensated downslope by compressional fold-and-thrust systems (Fig. 1a) (Damuth,1994; Corredor et al., 2005; Rouby et al., 2011).This study covers an area of 6200 km^2 on the southern lobe of the Niger Delta and incorporates a range of structures from the compressional domain, including a strain partitioning transfer zone (Fig. 2a). The northernmost part of the dataset images basinward-verging folds and thrusts of the inner fold-and thrust belt (Fig. 2a). The thrusts do not propagate to the surface, but their associated folds deform the seabed. The south-west of the study area is dominated by closely spaced, fault-propagation folds of the outer fold-and-thrust belt. The folds have hinge lines which strike NW-SE, perpendicular to the regional slope, with forelimb and backlimb synclines adjacent to the fold crest. The growth history of this region of the outer fold-and-thrust belt has recently been quantified by Pizzi et al. (2020). The thrust faults (associated with folds A-I; Fig. 1b) are shown to have started growing at ~15 Ma. Strain rates were initially slow (average strain rates < 200 m/Ma), increased significantly between 9.5-3.7 Ma (200-400 m/Ma), and then decreased in the last ~ 4 Ma to < 150 m/Ma, with many of the thrusts becoming inactive. Importantly for this study, Pizzi et al. (2020) use the well-constrained strain rates to demonstrate that strain varied spatially, between structures and along strike, and also through time, with marked variations in strain across adjacent structures over timeframes down to 1-2 Ma.

Finally, a complex, N-S trending strike-slip fault zone transects the study area, oblique to the regional slope dip. Features associated with the structure can be observed on the present-day seafloor where a series of en-echelon, extensional faults form a small pull-apart basin (Fig. 1b). The normal faults forming the basin trend NNW-SSE—oblique to the major N-S fault—and systematically offset the trace of the fault.

4. DATASET AND METHODS

4.1 Seismic Data and Interpretation

A time-migrated, 3D, seismic-reflection dataset was provided by Petroleum Geo-Services (PGS). The data were migrated using Kirchhoff pre-stack migration and bending ray post-stack migration to generate a 12.5 m by 12.5 m grid with a 4 ms sampling interval, which constrains the maximum horizontal resolution. The data were processed to near zero-phase and are displayed using SEG-normal polarity with a positive amplitude or peak representing an increase in acoustic impedance. The average frequency of the full-stack data is 50 Hz, resulting in a vertical resolution of approximately 7.5 m (assuming vertical resolution is equal to a quarter of the wavelength) using an average interval velocity of 2000 ms^{-1} (Morgan, 2003).

Seismic-reflections within the channel and overbank were mapped across three structural domains and from water depths of ~190 to 2,850 m. Four horizons (horizons 1-4) were mapped within the larger channel one system, and three within channel five (horizons 5-7) (Fig. 4). Seismic-reflection surfaces were chosen based on their stratigraphic relationship within the channel complexes (base, middle, upper, top) to capture the evolution of the system and constrain attribute maps. Individual terrace bases were mapped locally in channel one to interpret the deposit and the processes that formed the foundation of the terrace. Amplitude extractions were used alongside frequency decomposition maps (*see section 4.2*) to determine the planform configuration of channel elements. Seismic sections, taken ca. 2 km along the channel length, were used to interpret cross-sectional architectural changes down system and were correlated with planform maps to determine channel element centrelines. The mapping of individual channel elements within the two systems allowed channel centrelines to be reconstructed and sinuosity development to be analysed.

We interpret the high-amplitude, discontinuous reflections to be coarse-grained channelised deposits and chaotic, variable-amplitude, highly discontinuous reflections to be mass-transport deposits based on seismic-facies models of deep-water depositional systems (Posamentier & Kolla, 2003; Mayall et al., 2006). Overbank levee deposits were identified through their continuous straight reflections that converge and dim away from an associated channel. The base and top of levee packages were mapped and isopachs created. To evaluate the extent to which bathymetry relating to a structure was antecedent, preceding the channel, or active during the channel's evolution, we followed the method of Clark & Cartwright (2011) in using seismic-reflection termination relationships within the external levees (see *figure 3* Clark & Cartwright, 2011).

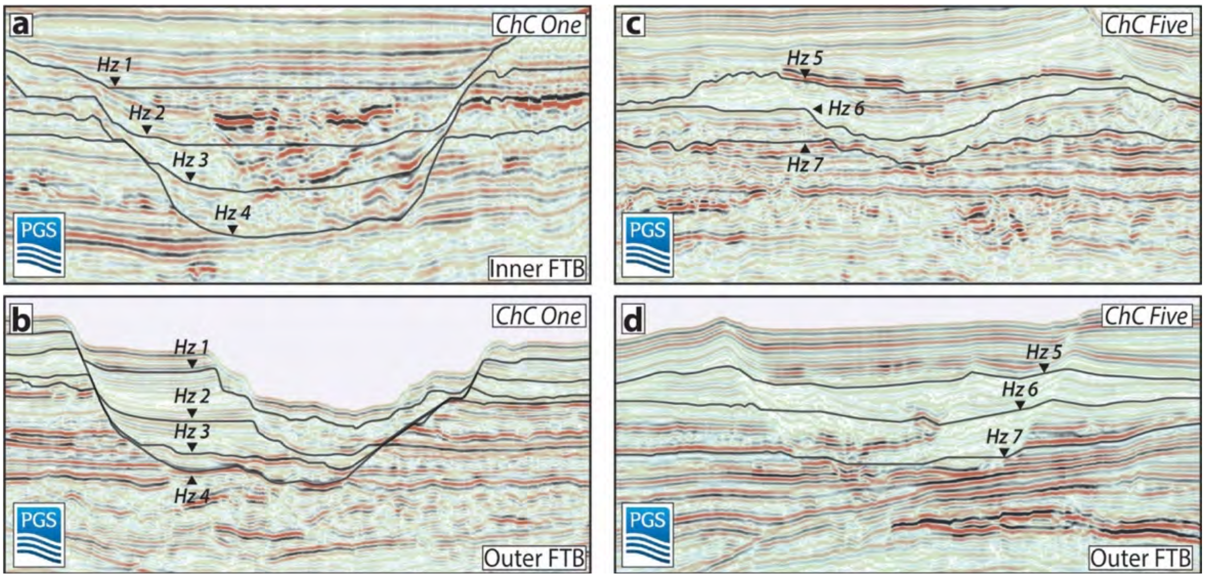

Figure 4. Seismic sections through channels one (a-b) and five (c-d) across the inner and outer fold-and-thrust belts. Horizons were mapped within the two channel systems and their overbank facies to capture the planform architecture of the systems and constrain attribute maps.

4.2 Frequency Decomposition and RGB Blending

Frequency decomposition combined with Red Green Blue (RGB) colour blending is a powerful imaging technique used to highlight features in seismic geomorphology (McArdle & Ackers, 2012). The seismic volume was decomposed into three frequency band-limited volumes with a different average frequencies: 24.28 Hz, 38.57 Hz and 53.85Hz. These volumes were assigned separate RGB colours (24 Hz = red, 38 Hz = green, 54 Hz = blue) and merged to produce a frequency colour blend. The colour hue in the blend reflects the average frequency around the studied horizon and the colour brightness represents the amplitude of the seismic signal. The blended frequency volumes were calculated using different frequency filter lengths (i.e. time intervals) so the visualized colour blend is a composite of three time windows centred around the chosen horizon. The resultant attribute is less sensitive to inconsistencies in the pick of a given seismic reflection than RMS amplitude extractions as it incorporates three time windows.

Here, frequency decomposition maps are used to interpret the planform morphology at multiple stratigraphic levels and consequently, allow the stacking of channel elements within the two systems to be determined at a regional scale (> 20 km along channel length).

5. STRATIGRAPHIC ARCHITECTURE OF THE NIGER DELTA CHANNEL SYSTEMS

We present results for channel systems one and five across the unstructured slope of the translational domain and the structured slopes of the fold-thrust belts and the strike-slip fault zone. Seismic sections taken at key locations along the systems length demonstrate tectonically driven changes in cross-sectional architecture across a range of spatial scales from the fundamental unit, the channel element, to channel complex set. Planform architectural changes are illustrated through a series of attribute maps (RMS amplitude and colour blended frequency decomposition maps).

5.1 Architecture of Channel System One

5.1.1 Strike-slip Fault Zone and Inner Fold-and-Thrust Belt

In its uppermost reaches, where deformation of the inner fold-and-thrust belt dominate, channel one is infilled and lacks present-day geomorphic expression. The system trends north-south along the strike of the strike-slip fault zone (Fig. 5a, 6a). The architecture is erosional, lacking external levee deposits, with surrounding reflections truncated against steep margins (Fig. 5a). In planform, evidence of channel element migration is limited as the system is constrained laterally by extensional faults associated with transtension in the fault zone. In section, the complex bounding surface, up to 3 km wide, 330 ms thick, and flat-based, confines vertically-stacked, high-amplitude channel elements which dominate the internal fill (Fig. 6b-c). The relationships between individual channel elements are complex, although, features associated with past entrenchment and erosional terrace formation can be inferred.

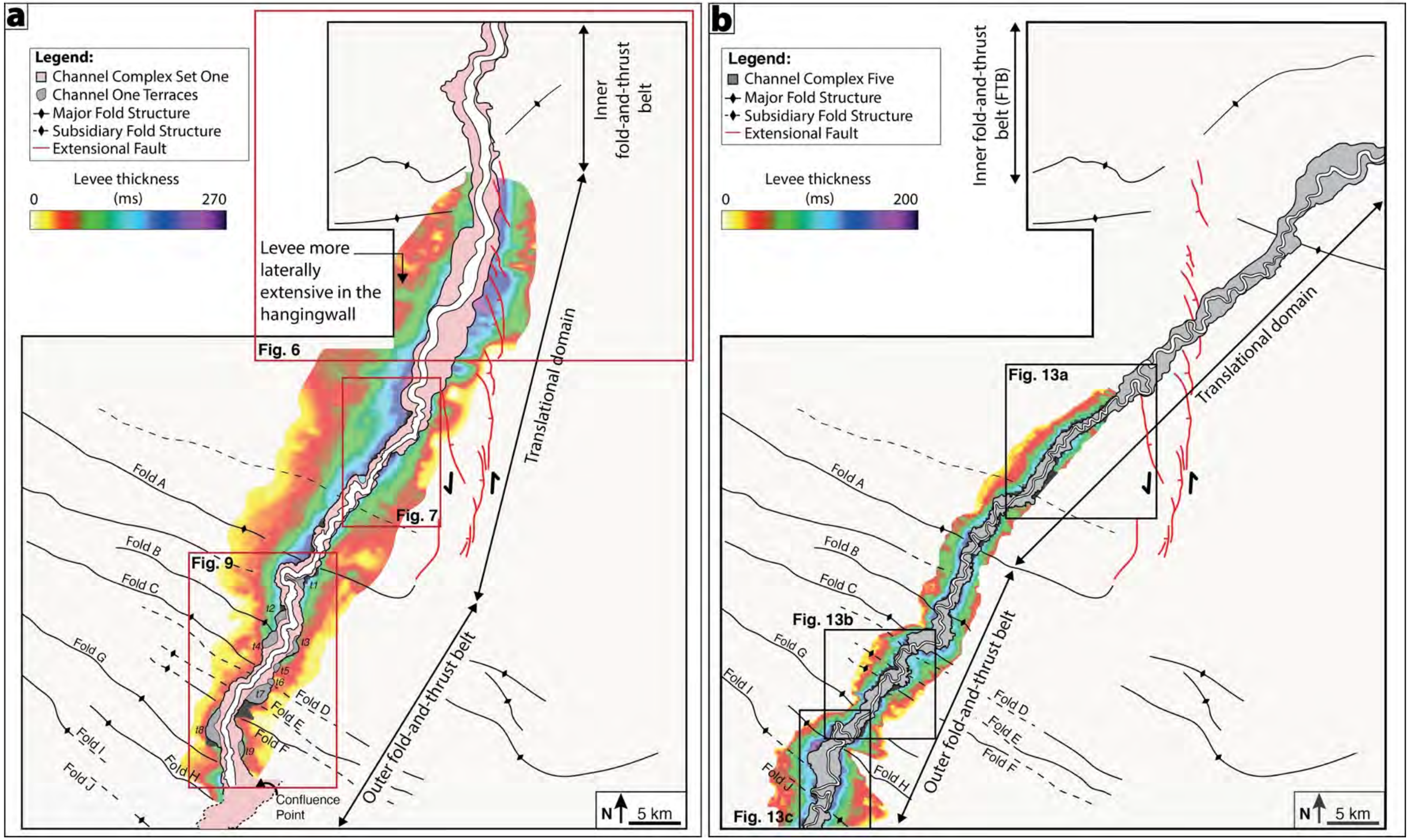

Figure 5. Line drawing of channels one (a) and five (b) showing the location of key geomorphic features including the final channel element within each channel complex, the location of terraces and terrace numbers within channel one, and the location of structural features such as thrust-folds and extensional faults of the strike-slip fault zone.

254

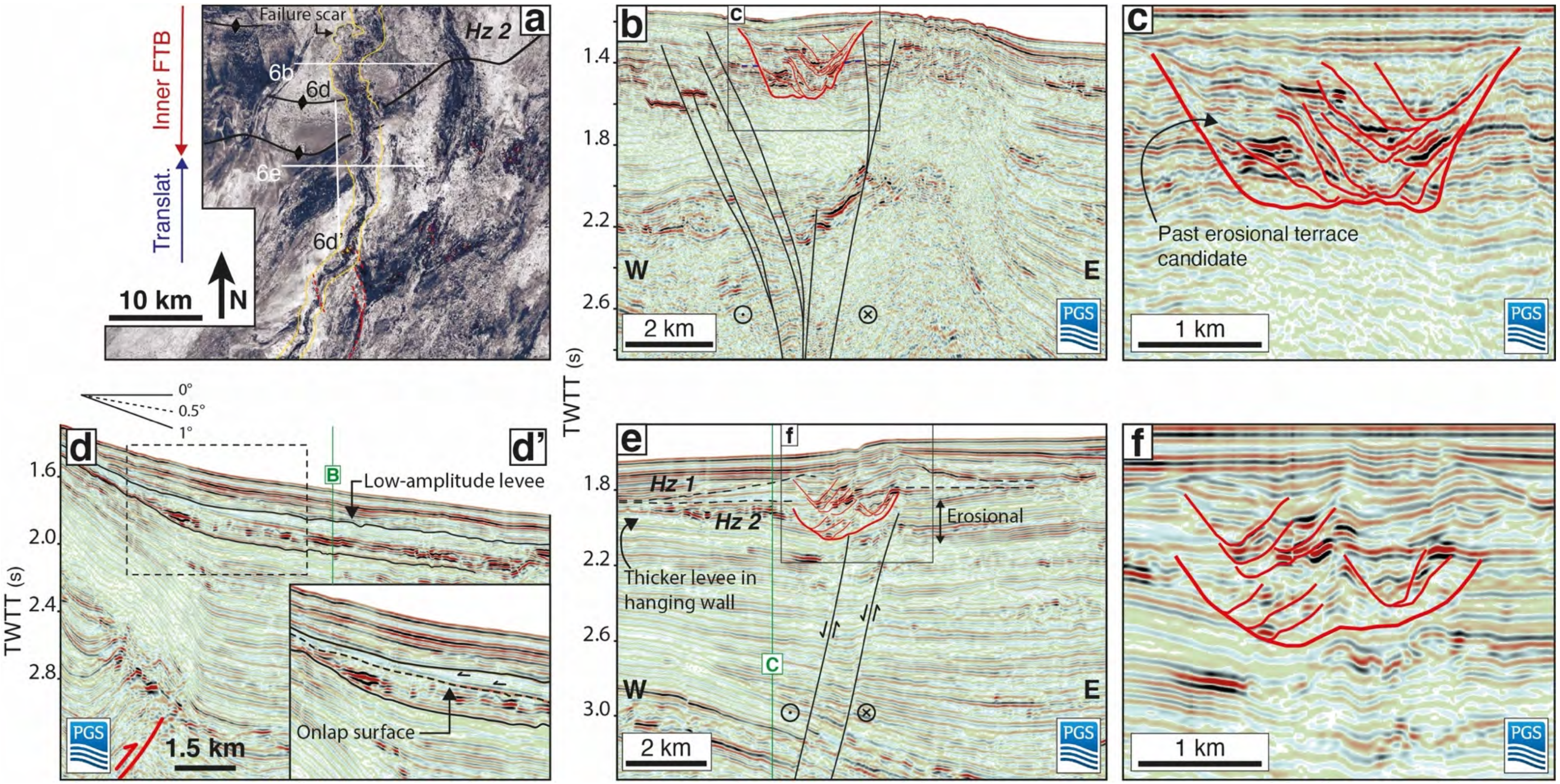

a
Failure scar
Hz 2
6b
6d
6e
6d'
Inner FTB
Translat.
10 km
N
b
c
W
E
1.4
1.8
2.2
2.6
2 km
PGS
c
Past erosional terrace candidate
1 km
PGS
TWTT (s)
0°
0.5°
1°
d
d'
B
Low-amplitude levee
1.6
2.0
2.4
2.8
TWTT (s)
Onlap surface
1.5 km
PGS
e
f
Hz 1
Hz 2
Erosional
Thicker levee in hanging wall
C
1.8
2.2
2.6
3.0
W
E
2 km
PGS
f
1 km
PGS

Figure 6. (a) A seismic amplitude map showing channel complex one across the inner fold-and-thrust belt (extracted from mapped horizon three). The system trends north-south along the strike-slip fault zone (the associated extensional faults are shown in red). (b-c) Seismic sections illustrating the erosional architecture adopted by channel complex set one across the inner fold-and-thrust belt. (d) Seismic section illustrating the development of levees at a marked concavity in the slope profile associated with the forelimb of the leading thrust of the inner FTB; levees onlap onto the inner FTB. (e-f) Seismic sections taken across the upper translational domain illustrating the development of asymmetric levees relating to strike-slip fault zone.

5.1.2 Translational Domain

Across the middle and lower translational domain, the system develops significant geomorphic expression through a present-day channel (Fig. 1b). Channel one remains relatively straight across the upper translational domain, trending north-south parallel to the strike-slip fault zone and oblique to regional dip (Fig. 6a). System width and thickness range from 1.8-2.7 km and 230-300 ms, respectively. The principal change from the inner fold-and-thrust belt to the translational domain is the development of external levees between horizons one and three (Fig. 6d-e). Low-amplitude levee reflections are first observed at a marked concavity in the slope profile and are initially chaotic (possibly slumped) (Fig. 6d). Disparities in levee thickness and extent between the hanging wall and footwall indicate an extensional component of movement on faults within the strike-slip fault zone occurred alongside channel development (Fig. 6e). The degree of erosion along the channel complex base is markedly reduced over a short downsystem distance and the system becomes erosional-constructional.

Amplitude maps (of horizons two and three) reveal channel element sinuosity remained low over the majority of this reach (Fig. 7a). Evidence of major bend expansion is restricted to a single high-amplitude bend (Fig. 7a-b). A seismic section through the bend apex shows a structural high, away from which channel elements progressively stack. Deposits associated with channel element expansion continued to accumulate in this location until the system was abandoned (Fig. 7b-d). Downsystem of the high-amplitude bend, the complex exhibits multiple low-amplitude bends. Upstream from these low-amplitude bends, arcuate shapes displaying a high-amplitude seismic response, and trending parallel to the concave outer bend of the last channel element characterise downstream translation or ‘sweep’ of the bends (Fig. 7a).

External levee thickness and width increase to a maximum of ~215 m (ca. 260 ms Twtt) and 11 km, respectively (Fig. 5a). Mapped horizons two and three correspond to significant changes in levee distribution and provide a useful constraint on channel evolution. Horizon two marks a shift in the location of levee development and correlates to an aggradation event separating two stages of channel elements, each of which represents an individual channel complex (Fig. 8a-c). A low-amplitude mass transport facies, which can be traced regionally along the channel's length, dominates the lower fill (Fig. 8). The downstream movement of bend apices, characteristic of the system's planform, results in channel one maintaining a relatively simple cross-sectional architecture and stable width of ca. 2 km over this reach. The lower of the two complexes displays a consistent arrangement of horizontally-stacked channel element deposits transitioning into a stacking pattern associated with a higher aggradation rate (oblique or vertically-stacked channel elements) (Fig. 7c-d *interpreted black lines,* and Fig. 8). In the upper complex, channel elements are predominantly stacked laterally with little aggradation between successive elements (Fig. 7c *interpreted red lines* and Fig. 8).

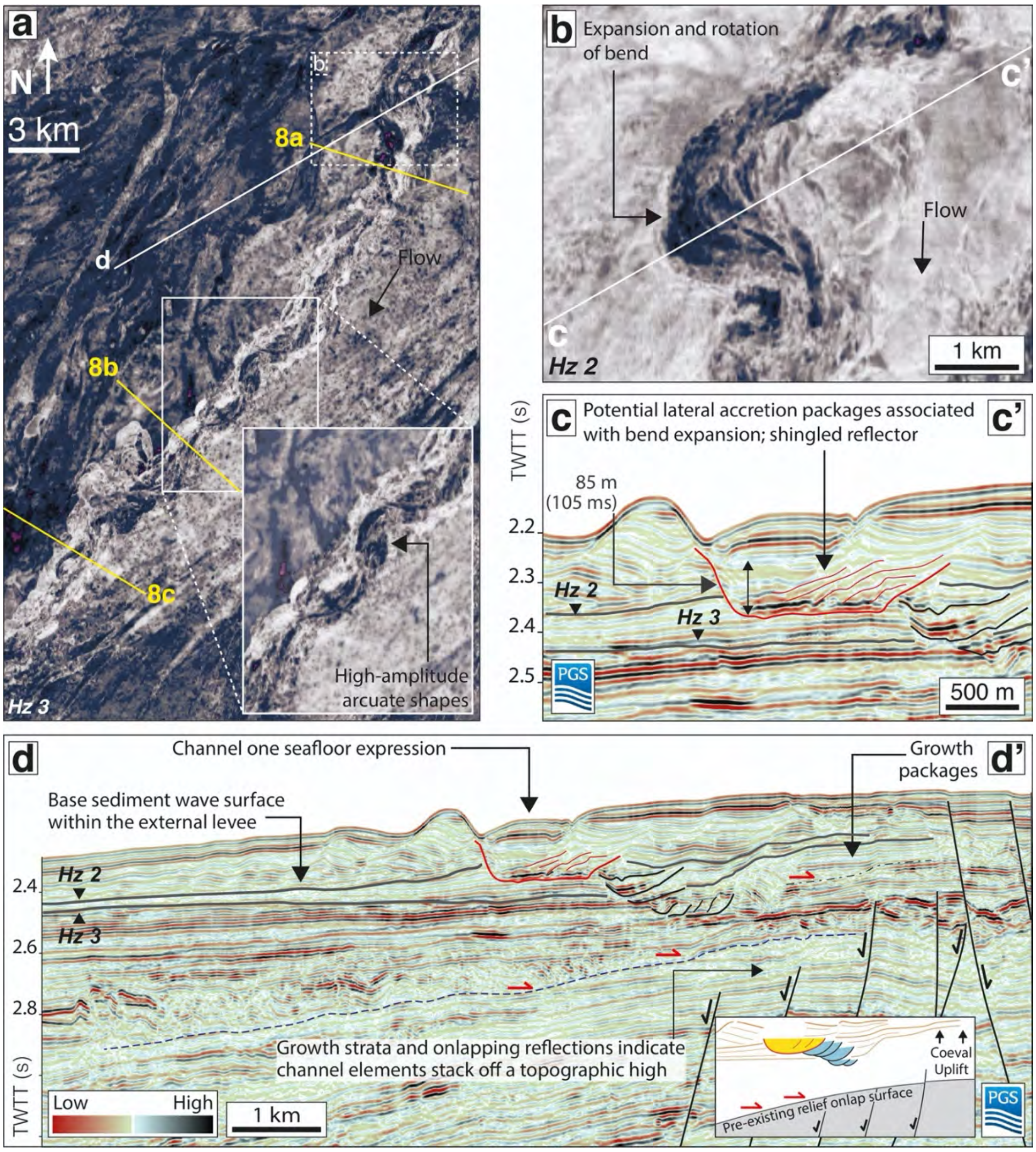

Figure 7. RMS amplitude maps in the middle and lower translational domain, showing: (a) the low-amplitude translating bends (with a high-amplitude seismic response) which characterise the majority of the channel length across this structural domain, and (b) the expanding bend above a fault-controlled bathymetric high. (c) A seismic section taken through the apex of the expanding bend shows low-amplitude reflectors, parallel to the channel margin, stacking in the direction of the final channel element, forming a shingled reflection geometry. (d) A regional seismic line shows multiple channel elements stacking off a bathymetric high relating to the strike-slip fault zone. White lines show the location of sections (c) and (d). Yellow lines illustrate the location of seismic sections shown in figure 8.

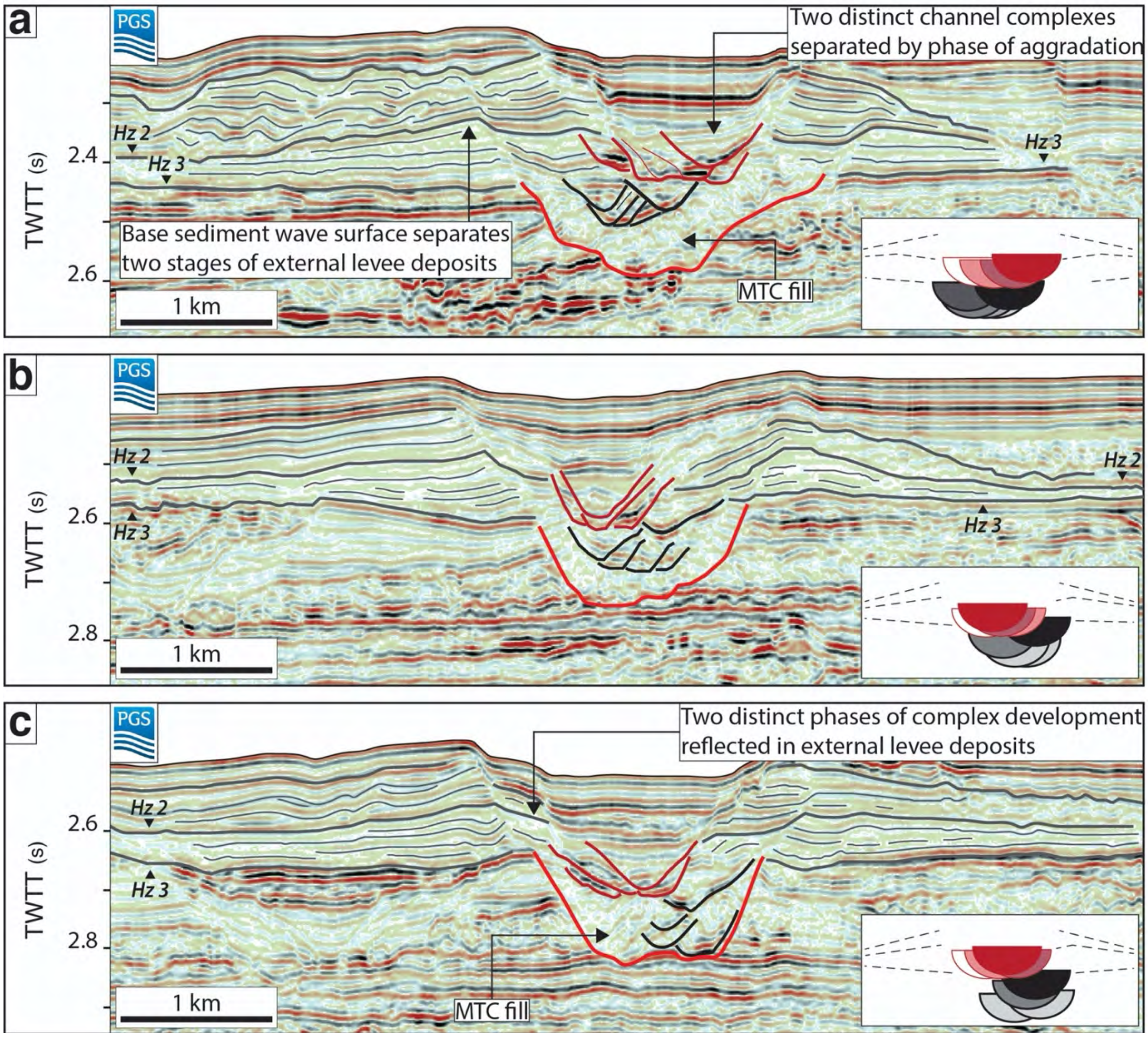

Figure 8. Seismic sections illustrating channel one's simple architecture across the middle and lower translational domain. The sections show channel element bounding surfaces within channel system one, the external levees confining the system, and the regional low-amplitude mass transport facies which dominates the lower fill. Mapped horizon two, the base of a sediment wave package, marks a significant shift in the location of levee development and correlates to an aggradation event separating channel elements of two stages within the system. The location of sections are shown in figure 7.

5.1.3 Outer fold-and-thrust Belt

Across the outer fold-and-thrust belt, channel one trends northeast-southwest interacting with fault propagation folds A-G, which form topographic ridges transverse to flow direction (Fig. 1b, Fig. 5a). The architecture changes from an erosional-constructional system confined principally by external levees to erosionally confined and ranges from wide and flat-based to narrow with steep margins and only minor external levees (Fig. 5a). The range of system widths increases to 1.8-4.4 km while the thickness range decreases to ~ 140-260 ms.

Amplitude maps illustrate a number of terraces across this structural domain (Fig. 9a). Terraces occur on both the inside and outside of the present-day channel bends, occurring between fold ridges (9 terraces in between 8 thrust folds). Amplitude maps reveal terrace bases to be primarily comprised of remnants of sinuous channel elements with evidence of meander expansion (Fig. 9c and 9d). High sinuosity channel element deposits typically occur up-dip of folds where the system is wide and amalgamate in a fixed position over fold crests (Figs. 9c). The base of terrace 1 (*t1*) is an exception exhibiting a chaotic discontinuous appearance consistent with a faulting and slumping into the channel (Fig. 9b).

In section, channel elements are the dominant seismic facies with localised mass transport deposits forming the secondary facies. The location of folds has a major control on the stacking of channel elements with large variability depending on the location relative to structure. Up dip of folds, where channel element deposits exhibit a high sinuosity planform, lateral stacking of successive channel elements is dominant and limited aggradation occurs (e.g., Fig. 10a, 10c). Proximal to the crest of folds the high degree of incision between channel elements of the lower and upper complex results in only partial preservation of channel elements of the lower complex and a decrease in complex thickness (Fig. 10b). Internal levees are restricted to wide, terraced sections of the system and are deposited interchangeably with flat, low amplitude terrace deposits. Due to the architectural complexity, channel system one's width (complex set scale) varies significantly over this channel reach linked with terrace development and tectonically driven changes in slope.

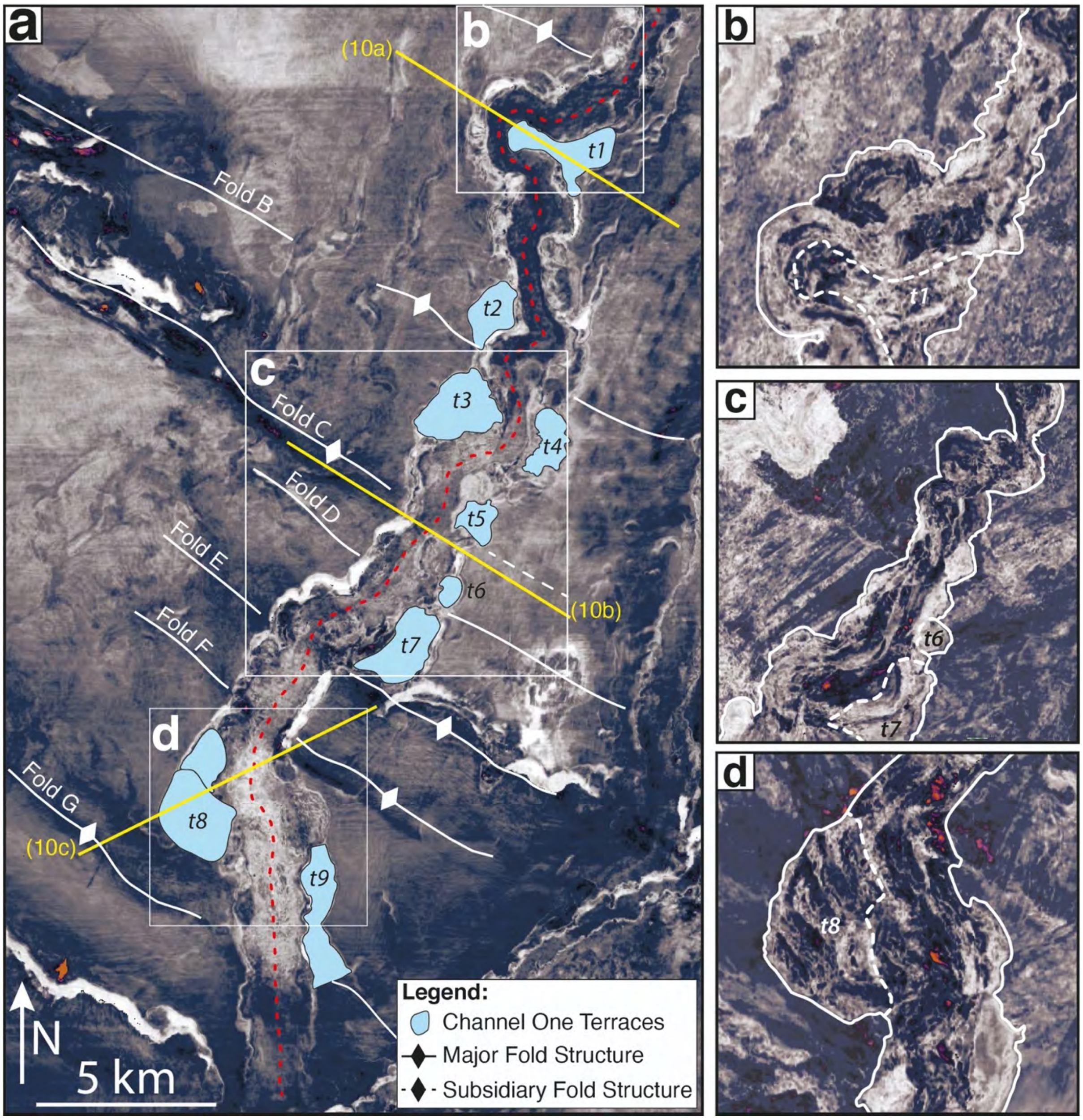

Figure 9. RMS amplitude maps from the present-day seafloor (a) and terrace bases showing the location of key geomorphic elements such as channel element deposits and the style of bend transformation (outer bend expansion and downsystem translation), terraces, and thrust folds across the outer fold-and-thrust belt. Light grey colour represents low-amplitude events, while dark and orange colours represent high and very high-amplitudes. The outline of present-day terraces are illustrated by dashed white lines on the amplitude maps. The present-day seafloor channel thalweg is shown by the red dashed line. Yellow lines indicate the location of sections shown in figure 10.

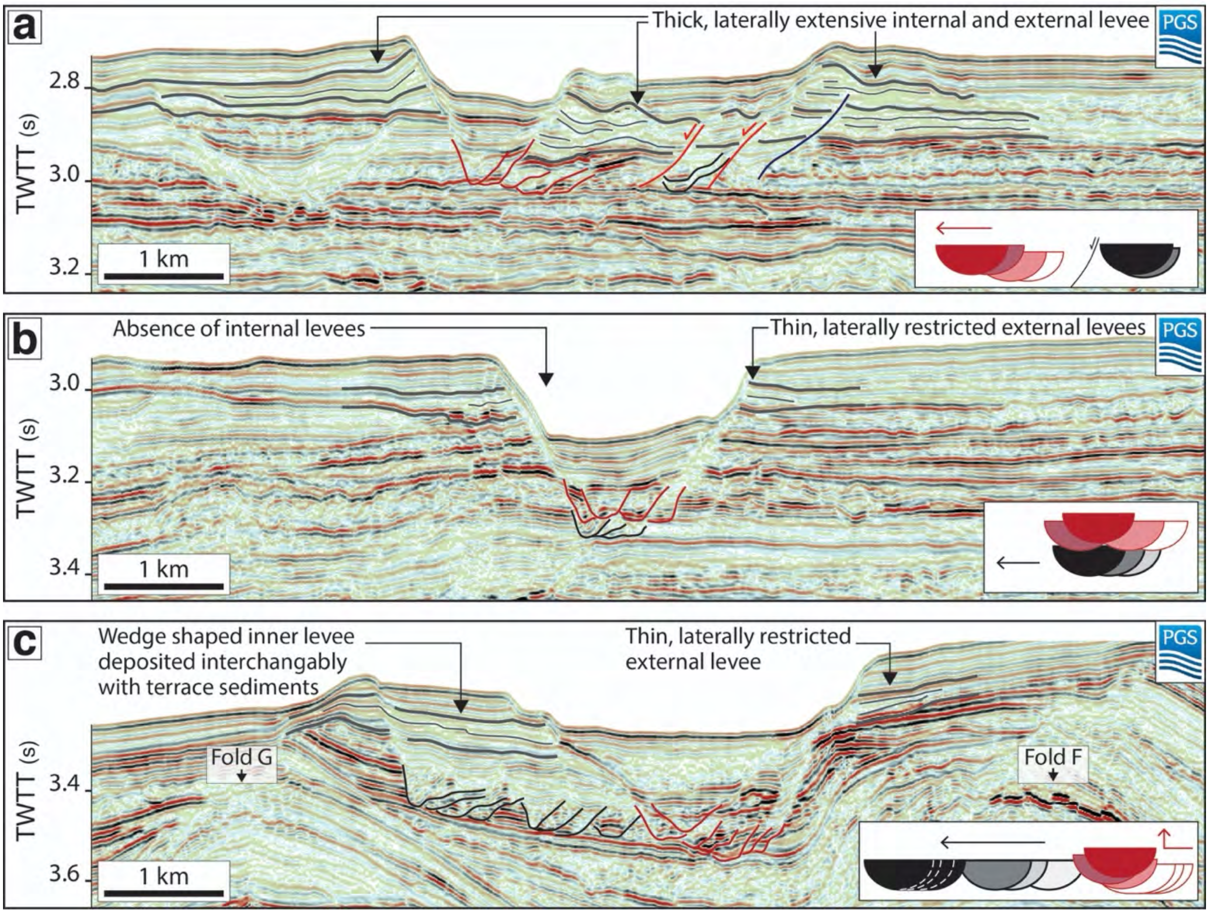

Figure 10. Seismic sections (a-c) illustrating the drastic change in channel-complex set architecture across the fold-and-thrust belt, including the stacking of channel-elements, the development of terrace bodies, and internal and external levee deposits. Sections (a) and (c) show the development of a wide channel system in between fold structures, while (b) shows the rapid narrowing of the system above the crest of structures. Sections (c) illustrate the horizontally-stacked channel elements which form the base of terrace 8 shown in figure 9.

5.1.4 Architectural Evolution of Channel System One at Element and Complex Scale

Channel one consists of two channel complexes, which through their constituent channel elements, provide a stratigraphic record of the competing processes of incision, aggradation, and migration. Horizon two marks the base of the upper complex as it incises into the underlying lower complex. A shift in the location of external levee deposition is concurrent with this stratigraphic horizon (Fig. 8).

Figure 11 illustrates the evolution of sinuosity of channel one regionally across the translational domain. The frequency map of horizon four records the earliest preserved channel elements of the lower complex and shows arcuate shapes parallel to the channel element outer bend associated with downstream translation (Fig 11a). This trend continues on horizon three with minor shifts in the location of bend apices between successive channel elements (Fig. 11b). Combined downstream translation and expansion sees several bend apices move oblique to flow direction (Fig. 11b). The base of the upper complex, horizon two, sees channel elements cut straight across the centrelines of elements of the lower complex with the exception of two high-amplitude bends which continue to expand (Fig. 11c). Horizon one records conformable stacking with horizon two and represents the final channel element prior to the systems abandonment and deposition of the hemipelagic wedge. Disconformity in channel element stacking between horizons two and three coincides with the abandonment of the lower complex and reincision of the upper complex and corresponds with the shift in location of external levee deposits.

In contrast, figure 12 shows the development of sinuosity in channel one across an area of the outer fold-and-thrust belt using colour blended frequency maps on horizons four and two, the bases of the lower and upper complex, respectively. Unlike the translational domain, channel elements of the lower complex have a localised region of high sinuosity characterised by tight, high-amplitude bends between folds D and E (Fig. 12a, c). Successive channel elements are organised, with bends transforming through both translation and expansion. Horizon two is again marked by channel elements cutting across the high-amplitude bends of the previous complex (Fig. 12c, d). The meander bend cutoffs generated form the foundation of present-day terraces (Figs. 9-10), such as the terrace up-dip of fold E (Fig. 12c-g). In locations proximal to thrust folds, channel element centrelines are relatively static forming a narrow system with a complex pattern of amalgamated channel elements (Fig. 12b).

In summary, the channel element sinuosity and the style and degree of migration are clearly sensitive to underlying structure. Downstream, translation is the dominant form of bend transformation recorded away from structure and across the translational domain (Fig. 7a, 11); cutoffs (Fig 9c, d, 12), expanding bends (Fig. 7b, 12), and accretion surfaces (Fig.7c, 12) are all restricted to reaches impacted by underlying structure. Consequently, stratigraphic architectures are increasingly complicated in locations of structure at the channel complex set scale

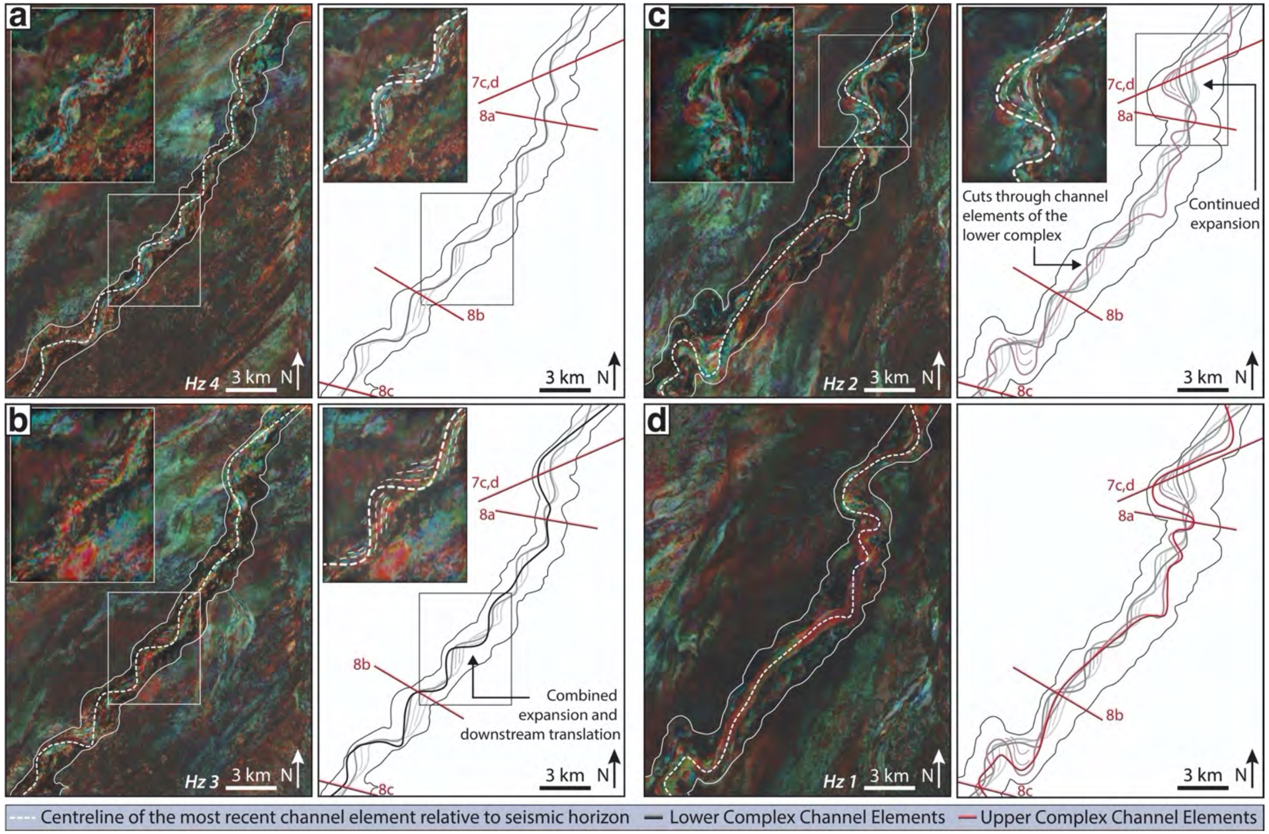

Figure 11. Colour blended frequency decomposition maps of the four horizons in channel one. Interpretative line drawings show the evolution of sinuosity at regional scale across the translational domain; interpreted channel element stacking compiled from the base horizon (Hz 4) to the most recent horizon 1 (Hz 1). (a-b) Illustrate the downstream translation of bend apexes between successive stacked channel elements of the lower complex. (c-d) Show the abrupt change in channel element organisation between the lower and upper complexes reflecting the abandonment and plugging of the lower complex's depositional relief.

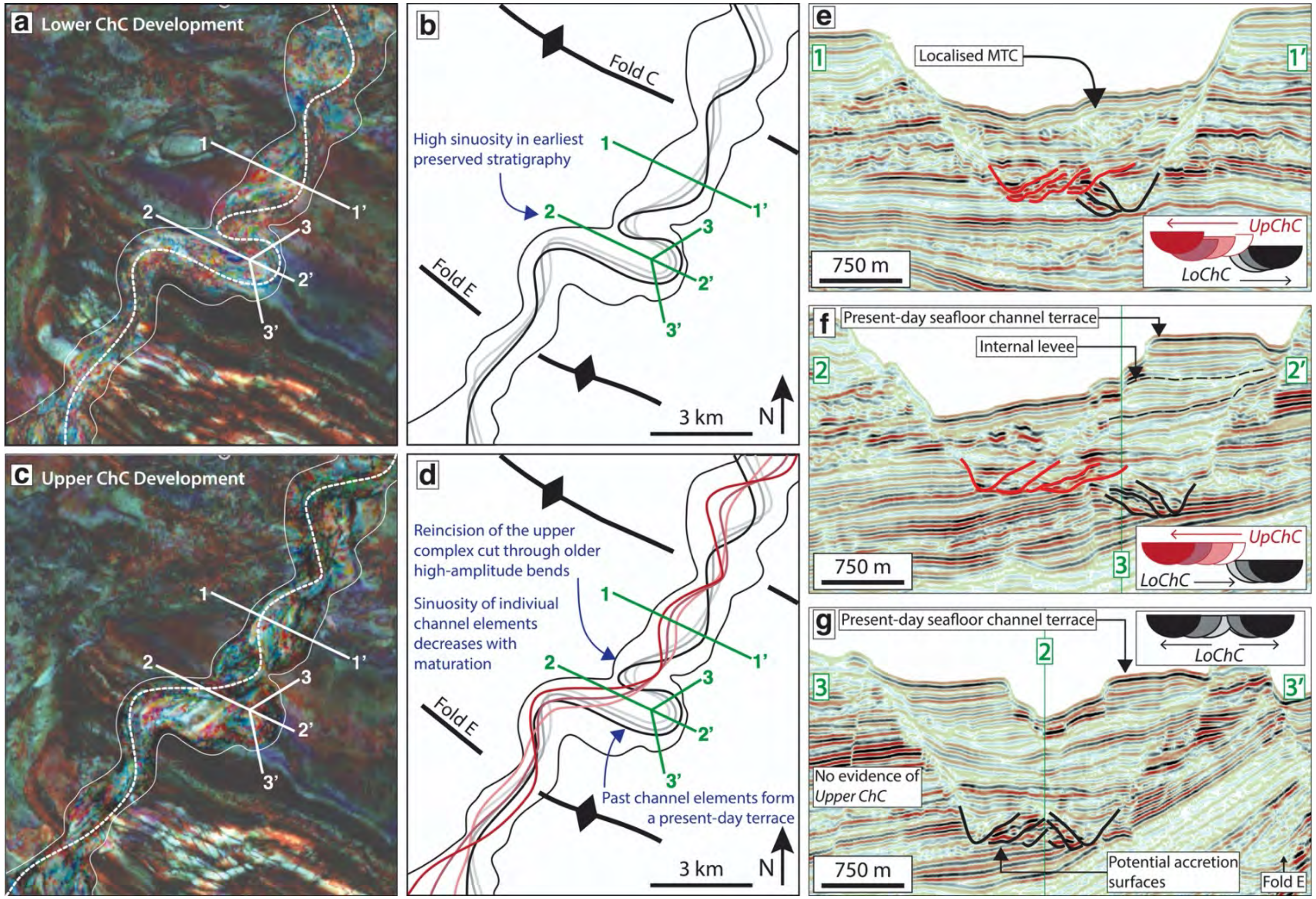

Figure 12. Frequency decomposition maps (a & c), line drawings (b & d), and seismic sections (e-g) illustrating the evolution of sinuosity and the development of bends across the fold-and-thrust belt. (a-b) Channel element sinuosity in the lower complex is high with a tight, high-amplitude bend preserved in several channel element deposits immediately up-dip of fold E. (c-d) Channel elements of the upper complex incise into the lower complex, generating a cutoff up-dip of fold E, which forms the base of a present-day terrace (f-g).

5.2 Architecture of Channel System Five

Channel five is the smaller and older of the two systems. Unlike the more recent channel system one, channel five does not pass across the uppermost slope and the inner fold-and-thrust belt within the study area. It is fully filled allowing the final channel element, prior to the system's abandonment, to be mapped for over 150 km (Fig. 5b).

5.2.1 Translational Domain and Strike-slip Fault Zone

Channel five initially trends northeast-southwest, down regional dip (Fig. 5b). The system has an erosional to constructional architecture with narrow aggradational levees (Fig. 5b). The dominance of mass transport deposits makes mapping and interpretation of internal and external architectures complex over this reach. Significant changes in complex architecture occur within the pull-apart basin associated with the strike-slip fault zone. Complex width and thickness increase up to 3.7 km and 165 ms, respectively. In planform, the final channel element is characterised by high amplitude bends (up to 2 km in width) with evidence of bend transformations through combined expansion and downstream translation (Fig. 13a). In section, this channel reach is characterised by channel elements which stack systematically toward the direction of the expanding bend, with significant aggradation between successive elements (Fig. 14a). Basal erosion increases markedly passing into the footwall of an easterly dipping extensional fault of the strike-slip fault zone before declining alongside complex width, channel element sinuosity, and bend amplitude with increasing distance from structure (Fig. 13a and d).

Across the middle and lower translational domain channel five has a simple erosional:constructional architecture. Low-amplitude, long-wavelength bends characterise the majority of the system length (Fig. 13a). Discontinuous channel element remnants, which cannot be traced for a significant distance downstream form a substantial part of the lowermost fill with arcuate shaped seismic-reflections, parallel to final channel element's low-amplitude (outer) bends, recording downstream translation (Fig. 13a). In section, channel elements fill the erosional component and are typically stacked laterally in the lower fill with aggradation increasing in the late stage of the system's evolution (Fig 14b-d). External levee thickness remains relatively consistently at around 100 m (130 ms TWTT) and extends laterally up to 5 km but is highly asymmetric due to erosion of the eastern levee by channel one (Fig. 3b).

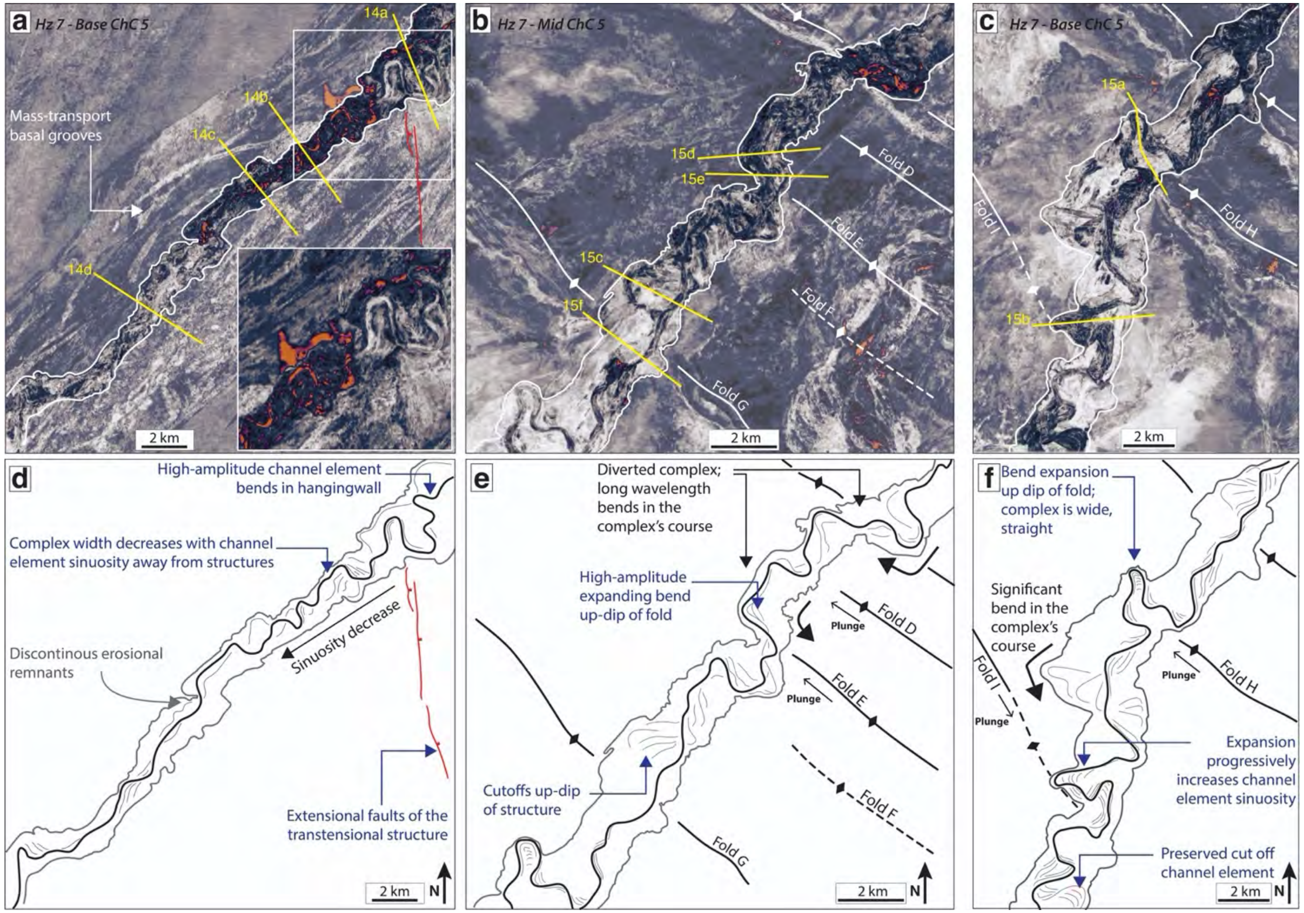

Figure 13. RMS amplitude extraction from (a) the translational domain, (b) folds C, D, E, F and G, and (c) folds G, H and I for channel complex five. Figure 13a shows the high sinuosity associated with extensional faults of the N-S trending transtensional fault zone; sinuosity decreases downsystem as structural influence decreases. Figures 13b and 13c show the increase in sinuosity at channel element and channel complex scale associated with variable uplift across the outer fold-thrust belt.

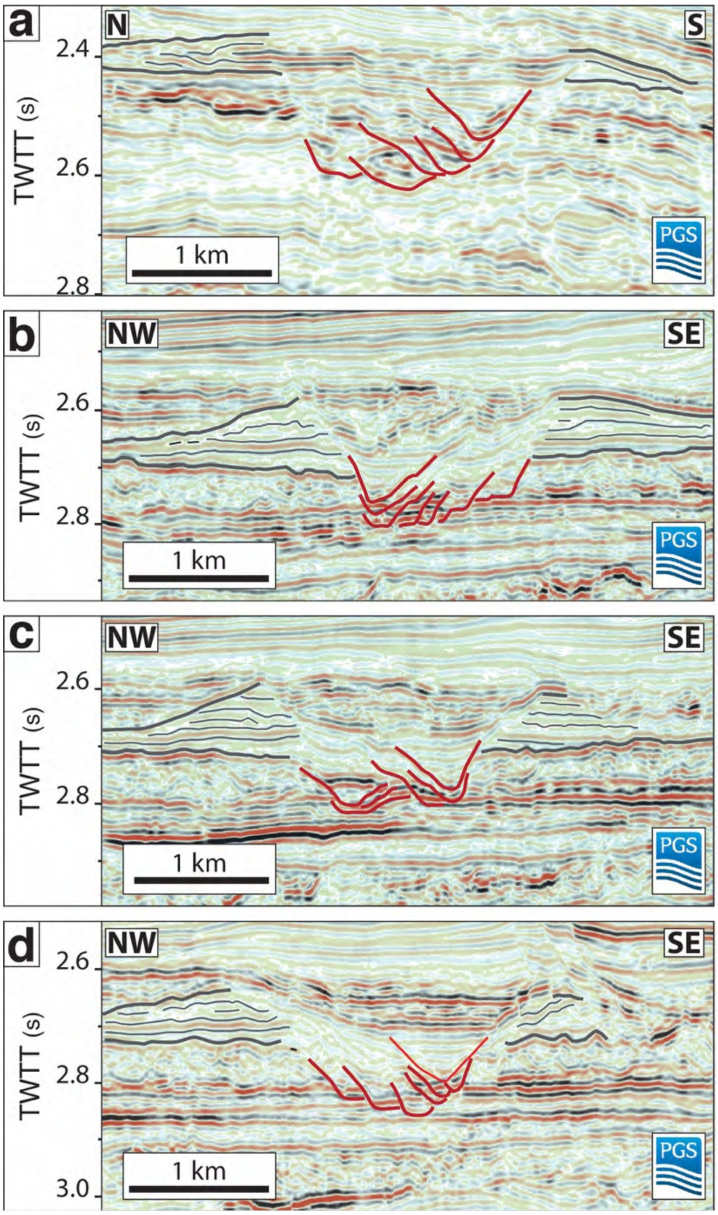

Figure 14. Seismic sections of channel complex five in (a) the hangingwall of an extensional fault associated with the strike-slip fault zone, and (b-d) across the unstructured, translational domain. Section (a) illustrates the erosional nature of the complex in the hangingwall with only thin external levees and the high aggradation stacking of successive channel elements toward the expanding bend shown in fig. 13a. Sections (b-d) show horizontally-stacked channel elements fill the erosional component of the complex and transition into an oblique to vertical stacking pattern in the later stages of complex development.

5.2.2 Outer fold-and-thrust Belt

Channel five undergoes significant changes across the outer fold-thrust belt, with systematic variations in architecture, channel element morphology and complex dimensions associated with the bathymetric template created by folds A-I. The complex itself has a sinuous morphology proximal to several folds (D, E, and I) with long wavelength bends forming in the direction of the associated fold's plunge (Figs. 13b and 13c). Complex width and thickness vary significantly, ranging from 1.2-3.9 km and 120-230 ms, respectively. Amplitude maps from the base of the complex display high sinuosity channel element deposits with features associated with meander expansion and increasing channel element sinuosity typically occurring up-dip of thrust folds where the complex is wide with asymmetric margins (folds C, H and I) (Figs. 13b and 13c). High sinuosity channel elements typically undergo bend expansion where the complex changes course (Fig. 13b). Over the crest of folds, the resolution of planform architectures is poor as the high-amplitude channel deposits narrow and amalgamate.

Figures 15a and 15b show sections taken through the apices of high-amplitude bends found up-dip of folds H and I, respectively, and illustrate the formation of a wide, thin complex with organised, horizontally-stacked channel elements up-dip of structure. Aggradation between successive elements is minimal. However, seismic sections across channel reaches between folds illustrate an organised stacking where horizontal-stacked channel elements dominate the lower fill before vertically-stacked channel elements dominate the latter stage (Fig. 15c). Figure 15d shows a section through a bend apex immediately up dip of fold D with a similar stacking pattern of horizontally-stacked channel elements climbing into vertically-stacked deposits. In contrast to up-dip of folds H and I, aggradation between channel elements is well represented up-dip of fold D by vertical stacking in the latter stages of complex development. Over the crest of folds, the stacking of channel elements is disorganised with evidence of significant reincision between channel elements (Fig. 15e, 15f). The distinct change in the organisation of channel elements with respect to structure results in marked fluctuations in the width of channel system five over the outer fold-and-thrust belt.

Levee thickness increases down system and is maintained across the outer fold-and-thrust belt (Figs. 5b, 15e, 15f). Localised variations in levee thickness relate to the presence of underlying folds and bends at channel element and complex scale, thickening at outer bends (Fig. 5b).

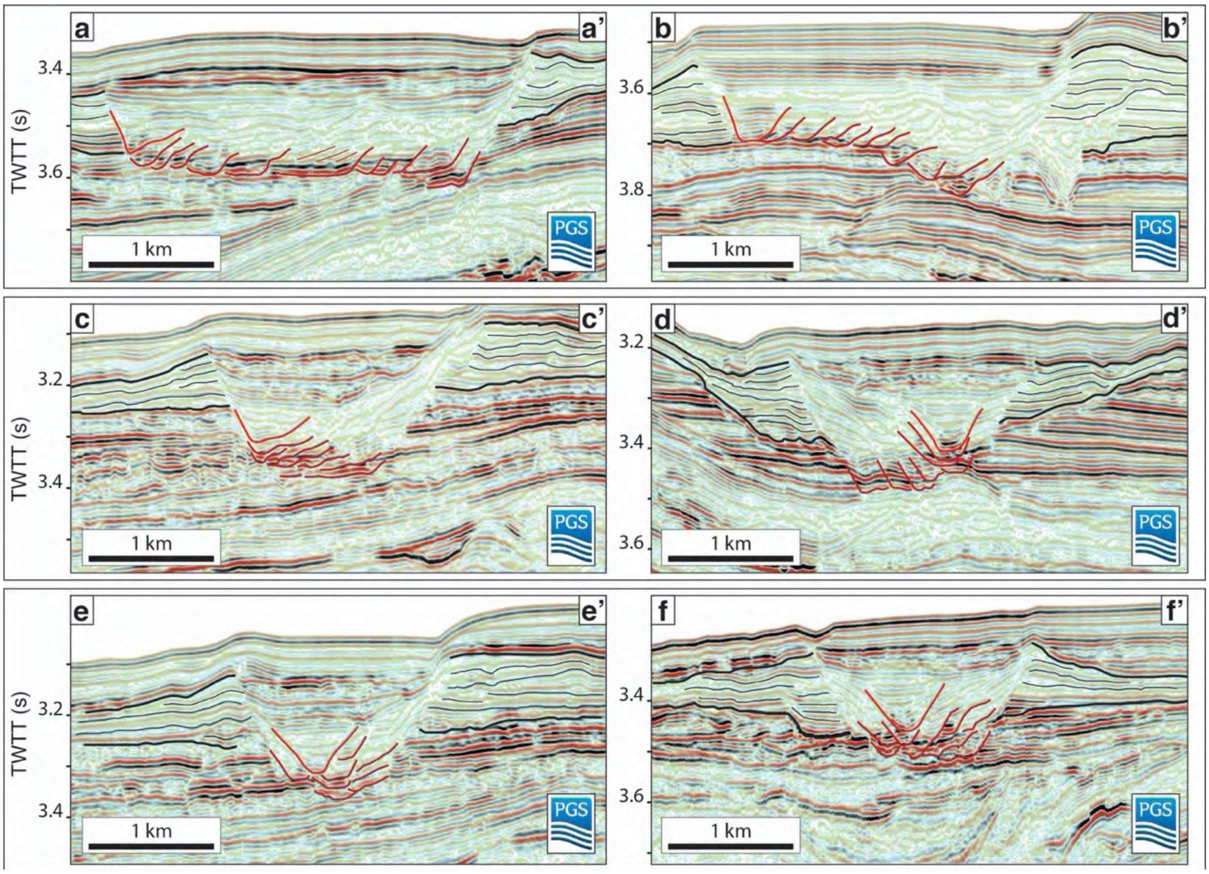

Figure 15. Seismic sections of channel complex five across the outer fold-and-thrust belt. Sections immediately up-dip (a, b, and d), in-between (c), or over the crest (e-f) of the underlying thrust-folds. See figure 13 for the location of sections and folds.

5.2.3 Architectural Evolution of Channel System Five at Element and Complex Scale

Figure 13 illustrates the change in channel element sinuosity, bend magnitude and the style and degree of bend transformation as the channel passes from the unstructured translational domain to the outer fold-and-thrust belt. Downstream translation is the dominant form of bend transformation away from structure across the translational domain (Fig. 13d). High amplitude, expanding bends and the generation of meander bend cutoffs are largely limited to areas influenced by underlying structure (Fig. 13e-f). As a result, planform architectures are increasingly complicated in locations of structure at the channel complex scale.

In section, the unstructured translational domain and channel reaches in between thrust folds in the outer fold-and-thrust belt structures are characterised by a two-stage evolution. An initial phase of organised horizontally stacked channel elements indicates early migration and bend development, followed by vertically stacked channel elements of the latter stage as the system aggrades (Fig. 14a-c, 15c-d). In contrast, in locations up-dip of folds where channel element sinuosity is enhanced due to the presence of structurally controlled bathymetry, aggradation between successive channel elements is negligible and sustained horizontal stacking indicates bend development continued into the late stage of the systems evolution (Fig. 15a-b).

Overall, channel five contains multiple genetically related channel elements that stack in a consistent, organised pattern connected by a single amalgamated surface and is interpreted as a single channel complex.

6. DISCUSSION

The two case studies above detail a number of channel-structure interactions across a range of spatial scales (channel element, complex, and complex set) and with a number of structures creating positive and negative relief. Several closely spaced fault-propagation folds of the fold-and-thrust belts produce complex bathymetries with linked positive relief (crests of the folds) and negative relief (from the associated the hangingwall and footwall synclines). Likewise, the strike-slip fault zone produces complex bathymetry with several positive relief structures along its length (e.g., Fig. 7d) in addition to the negative relief of the transtensional pull-apart basin. A systematic increase in the sinuosity of channel elements and the distribution of architectures associated with high sinuosity systems—cutoffs, terraces, and lateral surfaces—in locations with underlying structure is clear (*see sections 5.1.3 and 5.2.2*).

We use mapped levee seismic-reflection terminations to evaluate the extent to which the development of structurally controlled bathymetry predated channel inception. Subsequently, we characterise the planform and cross-sectional architectures adopted by the submarine channel systems based on their tectonic boundary conditions, setting out the morphological response from the fundamental architectural unit (channel element) up to channel complex set scale. Finally, we develop a conceptual model for the stratigraphic evolution of submarine channel systems under three different structural settings: unstructured, pre-channel structural bathymetry, and coeval structural bathymetry.

6.1 Relative Timing of Structural Deformation

Recent investigations into the growth history of fold-and-thrust belts have documented the temporal and spatial variation in strain across structures within the same belt (e.g., Totake et al., 2018; Pizzi et al., 2020). Folds of the outer fold-and-thrust belt initiated ~ 15 Ma and therefore predate the studied Pleistocene channel systems (Pizzi et al., 2020). However, many structures remain active, albeit at relatively low strain rates (< 150 m/Ma), while others became inactive between 6 and 3.6 Ma (Pizzi et al., 2020). Consequently, to characterise the response of the Pleistocene channels to structure, deformation must be considered over the time frame of a channel complex, to establish the extent to which bathymetry was antecedent or active during their evolution. While channel one has only thin, narrow external levees across the outer fold-and-thrust belt, channel five's external levees provide a useful constraint on the timing of relief development. Seismic-reflection terminations have distinct geometric relationships dictated by whether a structure is active, forming bathymetry, or inactive and bathymetry associated with pre-existing structure (Clark & Cartwright, 2011).

Figure 16 shows several seismic sections taken through channel complex five proximal to folds C, D, E, G and H. Where a structure was actively developing bathymetry during the evolution of the channel complex, the base levee seismic reflection is inclined and levee reflections onlap onto the surface (Fig. 16a-c; *folds C, G and H*). Continued uplift throughout levee deposition is recorded by the rotation and tilting of reflections (Fig. 16a-c). Where bathymetry associated with a structure predates the channel inception, levee reflections downlap or onlap at a low angle onto the base levee (Fig. 16d-e; *folds D and E*). Notably, the lack of progressive rotation and folding of early levee deposits indicates folds D and E were inactive during the development of channel complex five while folds C, G, and H were active.

6.2 Submarine Channel-Structure Interactions

6.2.1 Unstructured slopes

In planform, unstructured slope segments are characterised by channel elements exhibiting low-amplitude, long-wavelength bends (Fig. 13a). Upstream from these bends, arcuate shapes with high-amplitude seismic response, running parallel to the outer bend reflect the translation of the bends downstream (Fig. 7a). Downstream translation combined with minor expansion records slow progressive bend growth (Fig. 11b). The result is a channel complex of moderate width, mean width ~2 km, and with a relatively narrow range of widths along its length (Fig. 13a).

In cross-section, aggradation and migration are well represented in systems confined by well-developed external levees. Horizontally-stacked channel elements fill the erosional component of the channel complex and transition into an oblique to vertical stacking pattern in the later stages of complex development (Figs. 7a, 8b, 14b-d). This repeated arrangement of migration dominating the early stratigraphic record, and aggradation restricted to the latter suggests the rate of growth in channel complex width and the rate of change in sinuosity (bend development) relative to aggradation decrease throughout channel complex development. This model for channel complex evolution is in agreement with the two-phase model described by several authors (e.g., Peakall et al., 2000; Deptuck et al., 2007; Hodgson et al., 2011; Macauley & Hubbard, 2013; Jobe et al., 2016). The transition between the two phases, i.e., where migration predominantly ceases and vertical aggradation begins to dominate, likely marks the development of a stable morphology in which the flows are in equilibrium with the channel planform (see Peakall et al., 2000).

Where systems continue to develop beyond a single channel complex, the abandonment relief inherited from the most recently active complex is a principal control on the resultant stratigraphic architecture and the degree of conformity with underlying complexes (c.f. McHargue et al., 2011). In cases where abandonment relief is high, an organised stacking pattern will occur in which the path of the channel elements of the younger complex will approximate the path of the final element of the former complex. Channel one is an example where the abandonment relief of the lower complex was low at the time of reincision. The disorganised stacking pattern reflects the negligible influence of channel elements of the lower complex on the location and configuration of channel elements of the subsequent complex (Figs. 11, 12).

6.2.2 Structured slopes

While current models of submarine channel complex evolution (e.g., Peakall et al., 2000; Deptuck et al., 2007; Hodgson et al., 2011; Jobe et al., 2016) are valuable, their applicability to structured slopes is uncertain. Here, to develop our conceptual model for this setting, we use examples from channel complex five to illustrate the styles of channel-structure interaction observed. Figure 17 shows the stratigraphic architectures formed by channel five subdivided based on the principal controls dictating the system's response: the timing of channel inception, the relative timing of relief development, and the relief of the structure. Structural contours of the base complex (horizon 7) approximate structural bathymetry at the inception of channel five.

Pre-channel Structural Bathymetry

Where structural relief pre-dates the channel complex inception, the bathymetric template dictates the initial channel course i.e. early channel elements of the complex. Diversion of the channel, relating directly to the relief of the structure, may reflect the plunge or lateral variation in uplift of the underlying structure and results in long-wavelength bends in the channel complex such as those illustrated in figures 13b and 13c. Short wavelength bends at channel element scale appear superimposed on the diverted trend and transform locally via downstream translation or expansion toward lower bathymetry (Figs. 13b and 13c).

Figure 17a shows an example from channel five as it diverts around a bathymetric high created from folds D and E. Sinuous channel elements pass around the positive relief and toward a relative bathymetric low in the west, amalgamating to generate a sinuous form at channel complex scale. Higher frequency channel element bends, superimposed on the long wavelength diversion, transform locally via downstream translation (Fig. 17a bends intersected by *sections 1, 2, and 3*) or expansion (Fig. 17a bends intersected by *section 4*). Cross-sections show migration to be the dominant process early in the channel complex's development and aggradation in the latter (Fig. 17 *sections 1-4*). In reaches across positive structural relief, complex width and thickness are comparable to unstructured segments of the complex (Fig. 14b-14c and 17a *sections 3-4*). Where structure created a depression on the slope, complex width may be more significant, but a similar pattern of channel element evolution occurs with migration and changes in complex width occurring early in the complex's evolution (Fig. 16a *sections 1-2*).

Overall, where structural relief pre-dates channel inception the principal adjustment to the system is in the initial channel course, i.e. a planform adjustment, as early channel elements are forced around positive relief created by the structure. Cross-sections suggest the diversion of the channel course was sufficient for the system to evolve in a way comparable to an unstructured complex with bend expansion and migration occurring at an early stage, before a late stage where aggradation rate is high. Through this evolution, the system develops to a stable state of planform equilibrium and equilibrium width at which along channel length and complex width are maintained with continued flows (Peakall et al., 2000).

Coeval Structural Bathymetry: Positive Relief

Where positive structural relief and related synclines continue to grow as a channel complex simultaneously develops, the system responds by increasing channel element migration relative to aggradation creating a wide complex with high-amplitude channel element bends such as those observed up dip of folds C, H, and I (Figs. 13b and 13c). In contrast to diversion, the principal morphological adjustment is clear in both planform and cross-sectional architectures. In planform, a progressive increase in channel element sinuosity and the amplitude of bends developed occurs immediately up dip of folds, in the hangingwall (Fig. 13c). Increasingly sinuous channel elements amalgamate to generate a wide complex with highly asymmetric margins which narrow rapidly passing over the fold crest. In cross-section, channel element stacking departs from the patterns of the unstructured slope. Up dip of developing structures, where channel element sinuosity is at maximum, migration is the primary process recorded via horizontally-stacked channel elements (e.g., Fig. 15a and 15b). Aggradation, typically recorded in the latter stages, is either absent or heavily reduced.

Figure 17b illustrates high sinuosity channel elements of channel five as it interacts with interrelated positive and negative relief of fold H. Up-dip of the fold, successive channel elements translate downstream toward the bathymetric low of the hangingwall syncline before deflecting northwest and forming a tight, high-amplitude compound bend with smaller meanders superimposed. Channel elements exploit the asymmetry of the structure and progressively shift off developing relief in the east with the bend expanding into the relative bathymetric low of the hangingwall syncline (Fig. 17b). Complex margins are highly asymmetric, but complex sinuosity is low. Cross-sections up dip of the structure record migration through a series of horizontally-stacked channel elements (Fig. 17b *section 5*). Consequently, complex width increases locally by a factor of 2 whilst thickness is reduced by a factor of 1.5 (Fig. 17b *section 5*).

A key implication of coeval channel-structure interactions is that where structure is actively modifying the slope by creating positive relief, a channel complex will not reach planform equilibrium or width. Instead high-amplitude bends will continue to transform, increasing channel element sinuosity into the latter stages of complex development, with the phase of aggradation either being significantly subdued or absent altogether. The effect of this is that migration dominates the stratigraphic record.

Coeval Structural Bathymetry: Negative Relief

In the case where a structure is modifying slope morphology, developing negative relief coevally with complex development, the system responds by modifying the rate of channel element migration and aggradation. Locations of negative relief development, unrelated to the formation of a positive structure, will see the system adjust by progressively increasing channel element sinuosity and the amplitude of bends (Fig. 13a). Increasingly sinuous channel elements amalgamate to generate a wide complex with asymmetric margins. However, unlike coeval positive structures, the increase in channel element migration in negative relief is accompanied by a substantial increase in aggradation. In cross-section, oblique stacking of successive channel elements records continual migration and aggradation processes, developing a thick, wide complex.

An example of a channel-structure interaction with an active structure forming negative relief is channel five with an extensional fault of the strike-slip fault zone. Figure 17c shows a complex pattern of channel elements showing bend expansion combined with downstream translation, before channel elements deflect northward, parallel to the fault plane. The deflection is in direct response to along strike variations in throw with less relief in the north. Cross-sections show horizontally-stacked channel element deposits in the lower stratigraphy transitioning into an oblique stacking pattern in the complex's upper. This arrangement records continued migration throughout the complex's evolution even in the latter stages where the rate of aggradation increases relative to migration (Fig. 17c *section 6*). The increase in sinuosity between successive channel elements and the oblique stacking in cross section indicate the channel system has not reached a state of planform equilibrium; rather, channel elements bends continue to transform forming increasingly tight, compound bends and modifying complex width in the latter stages.

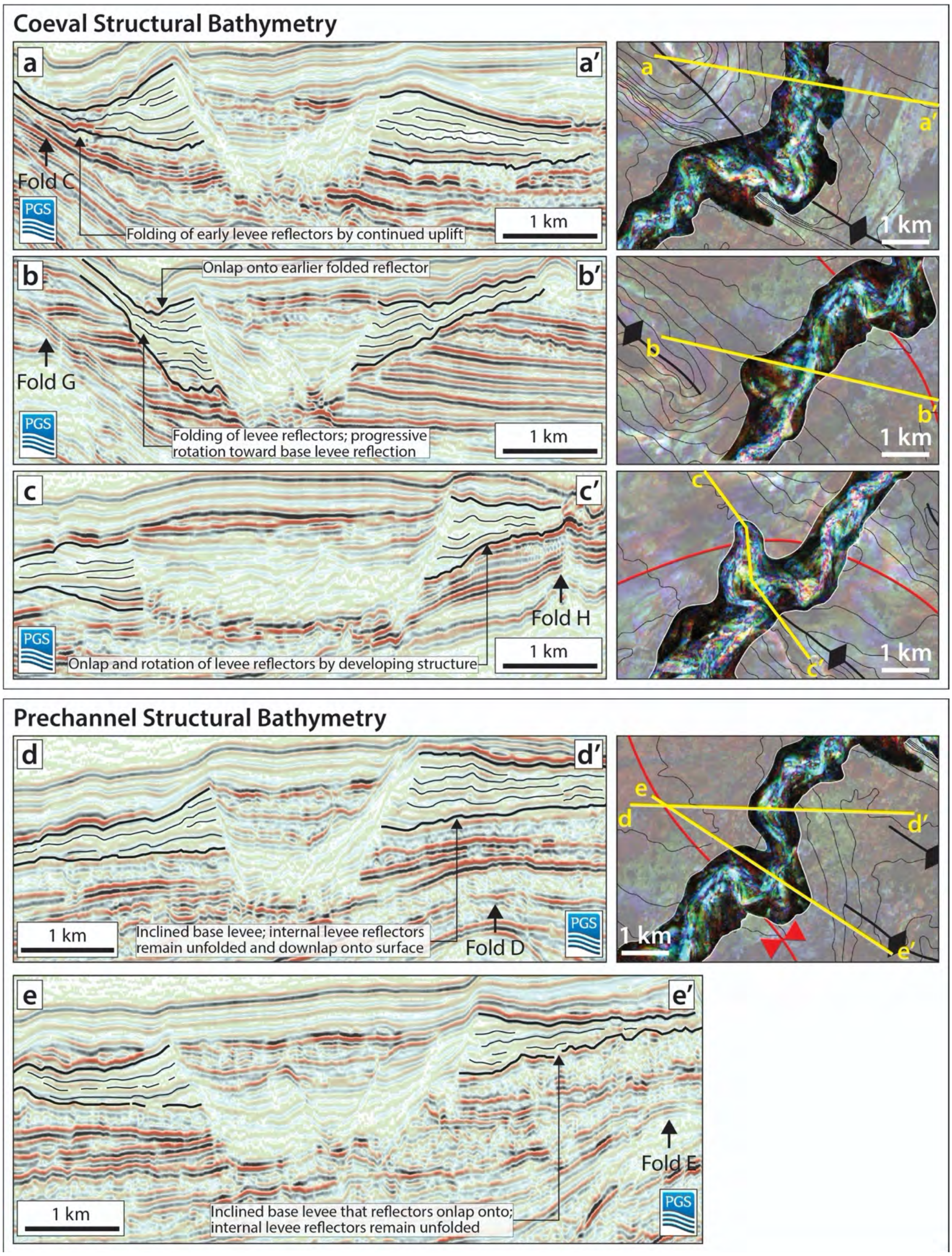

Figure 16. Seismic sections illustrating the seismic-reflection termination pattern for coeval (a-c) and prechannel (d-e) structural bathymetry. Levee reflections onlap onto the base levee and progressively rotate with continued folding during deposition i.e. coeval structural growth. Where structural bathymetry predates channel inception, levee reflectors gently downlap or low-angle onlap onto the base levee surface with no rotation.

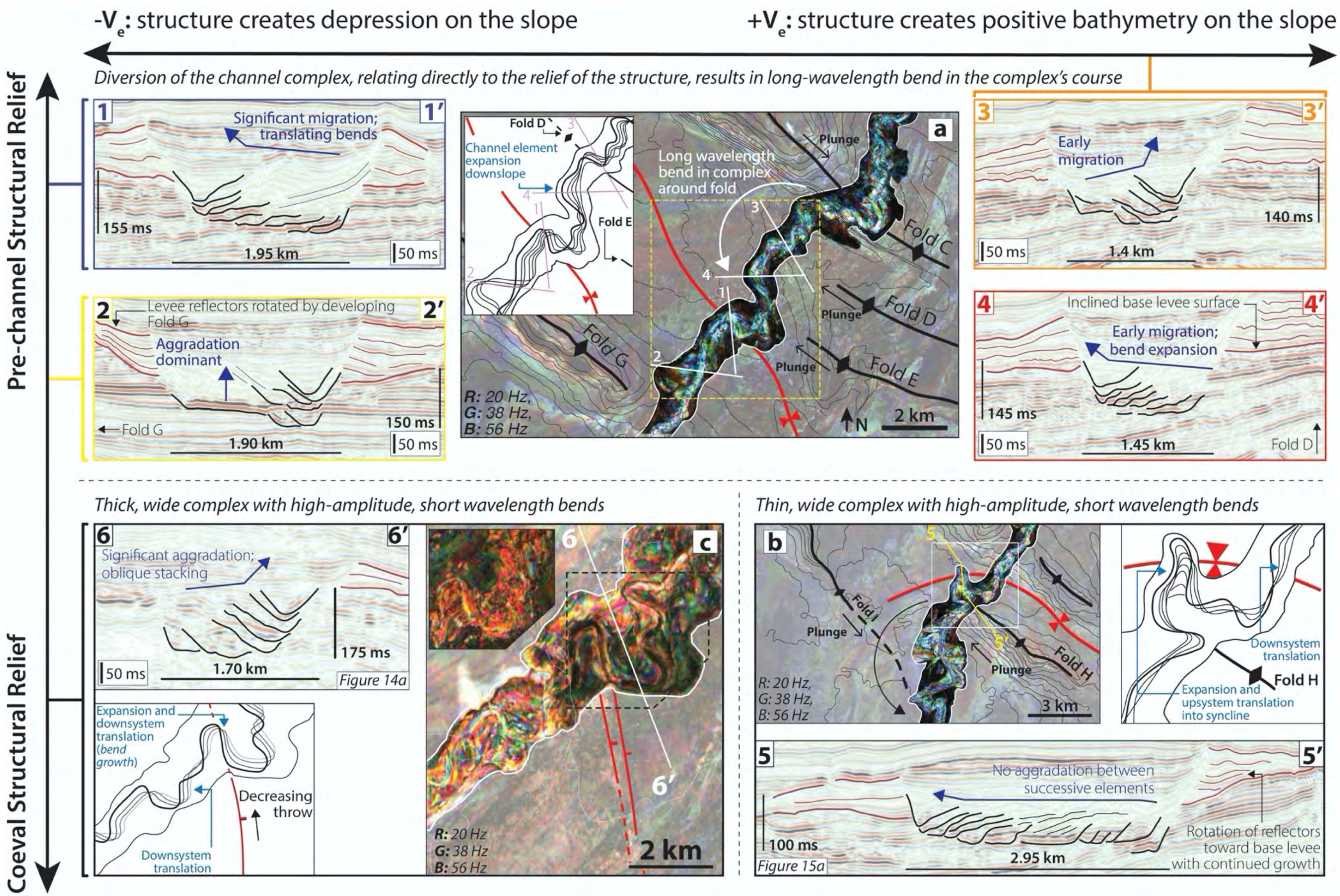
-Ve: structure creates depression on the slope
+Ve: structure creates positive bathymetry on the slope
Pre-channel Structural Relief
Coeval Structural Relief
Diversion of the channel complex, relating directly to the relief of the structure, results in long-wavelength bend in the complex's course
1
1′
Significant migration; translating bends
155 ms
1.95 km
50 ms
2
2′
Levee reflectors rotated by developing Fold G
Aggradation dominant
Fold G
150 ms
1.90 km
50 ms
a
Fold D
Channel element expansion downslope
Fold E
Long wavelength bend in complex around fold
Plunge
Fold C
Fold D
Fold E
Fold G
R: 20 Hz, G: 38 Hz, B: 56 Hz
N
2 km
3
3′
Early migration
140 ms
50 ms
1.4 km
4
4′
Inclined base levee surface
Early migration; bend expansion
145 ms
50 ms
1.45 km
Fold D
Thick, wide complex with high-amplitude, short wavelength bends
6
6′
Significant aggradation; oblique stacking
175 ms
50 ms
1.70 km
Figure 14a
Expansion and downsystem translation (bend growth)
Decreasing throw
Downsystem translation
c
R: 20 Hz
G: 38 Hz
B: 56 Hz
2 km
Thin, wide complex with high-amplitude, short wavelength bends
b
Fold
Plunge
Fold H
R: 20 Hz, G: 38 Hz, B: 56 Hz
3 km
Downsystem translation
Fold H
Expansion and upsystem translation into syncline
5
5′
No aggradation between successive elements
100 ms
2.95 km
Figure 15a
Rotation of reflectors toward base levee with continued growth

Figure 17. Examples of the stratigraphic architecture adopted by channel five to varying tectonic conditions. (a) Pre-channel structural relief (associated with folds D and E) results in diversion of the channel complexes course around positive relief. (b) Coeval positive relief $+v_e$ (vertical elevation) results in channel elements progressively expanding toward the relative bathymetric low of a hangingwall syncline, generating a wide, thin complex. (c) Coeval negative relief results in channel element bend expansion and a wide, thick complex.

6.3 Process and Stratigraphic Evolution Model

Based on the observed depositional architectures and the styles of channel-structure interaction, we develop a series of models for the formation of channel complex deposits and their composite bounding surfaces (Fig. 18). We interpret their formation via a complex-scale incision-to-aggradation cycle upon which a discrete number of element-scale incision and fill cycles are superimposed. Numerous studies have recognised stepwise incision, migration, and aggradation at channel element scale (e.g., Abreu et al., 2003; Mayall et al., 2006; Kolla et al., 2007), and complex-scale incision-to-aggradation trends (e.g., Deptuck et al., 2003, 2007; Kolla et al., 2007; Hubbard et al., 2009; Hodgson et al., 2011; McHargue et al., 2011; Sylvester et al., 2011; Jobe et al., 2015). However, the paucity of active turbidity data in natural systems (Paull et al., 2018), and the timescale of channel element/complex deposition (>10 Ky (e.g., Jobe et al. 2015)) means the full set of processes driving these two distinct scales of cycle remain poorly constrained. Here, we place current understanding in the context of the observations made from our studied channel systems, before we turn to the conceptual models themselves.

At channel complex scale, several processes have been proposed to explain of the cessation of incision and the onset of migration and subsequent aggradation. One well-documented hypothesis is changes in the properties of the channelised flows as the system develops (e.g., Mayall et al., 2006; Kolla et al, 2007; Jobe et al., 2015). An initial phase of erosion, associated with high energy, high discharge turbidity currents, forms a large erosional surface i.e., the complex bounding surface, and only deposits a thin basal lag (e.g., Mayall et al., 2006; Kolla et al., 2007). Subsequent reductions in flow volume and energy lead to under-fit flows which, over time, form sinuous channel networks that fill the erosive surface (Kolla et al., 2007). Further reductions in flow energy increase deposition internally, within the active channel element, and externally, in overbank settings (Peakall et al., 2000; Kolla et al., 2007). A positive feedback between levee growth and thalweg aggradation—where progressive overbank deposition leads to aggradation of the channel thalweg in order to maintain cross-sectional area—promotes aggradation and may limit the ability of channel elements to migrate laterally (Peakall et al., 2000; Jobe et al., 2016; Shumaker et al., 2018).

While we recognise a clear phase of late-stage aggradation and levee development, this model is not consistent with what is observed in the studied systems. The concept of large initial flows creating the erosional channel complex surface, which is then progressively filled is contrary to the formation of a wide, thin complex where structure develops positive relief simultaneously with channel development. If large initial flows were the principal process driving the development of a complex bounding surface there would not be distinctions in the architectures associated with active and pre-channel structural bathymetry and the surface would not be time transgressive**.** Instead, such architectures demonstrate multiple phases of modification and partial infill through cycles of incision and deposition forming a composite bounding surface. Additionally, the limited variability in channel element dimensions likely reflects a lack of significant changes in discharge and sediment supply (Sylvester et al. 2011). Therefore, changes in flow properties alone are not sufficient to develop the architectures observed; however, they may play a significant role in developing a state of relative planform equilibrium as we discuss below.

Other processes invoked to drive phases of channel complex development include changes in longitudinal profile (e.g., Pirmez et al., 2000; Hodgson et al., 2011), base-level change (McHargue et al. 2011; Sylvester et al. 2011, 2012), and changes in sediment supply versus accommodation space creation (Kneller, 2003). While these are difficult to reconstruct for individual channel systems, changes longitudinal profile provide a plausible explanation for the response of the channel systems to coeval structural bathymetry. Maintaining a longitudinal profile shape may drive the lateral expansion in response to the slope convexity associated with a developing positive structure. Additionally, where structure is actively creating negative bathymetry, the same process may drive the increase in aggradation throughout a system's development.

At channel element scale, a discrete number of cut and fill cycles is preferred to the continual migration of a single channel element (e.g., Sylvester et al., 2011) given observations of the dominance of horizontal seismic reflections filling erosive surfaces and the limited number of lateral accretion surfaces and shingled reflections observed (referred to as laterally stacked channel deposits (Abreu et al., 2003; Mayall et al., 2006; Kolla et al., 2007), or lateral step remnants (Kane et al., 2010)). Further work to constrain the processes remains an outstanding research objective and will require the integration of multiple data sources across a range of depositional timescales (flume tank experiments, outcrop studies, seafloor bathymetry and bathymetry time-lapse data, 3D seismic geomorphological and well data, and numerical models etc.). Nevertheless, a key implication of our results is the critical role the organisation of channel elements has on stratigraphic architecture at channel complex and channel complex set scale. Consequently, understanding the kinematic processes behind the discrete cyclicity of channel elements is critical to building an accurate model of submarine channel evolution and stratigraphic architectures.

Based on these considerations and our results, we have developed a general four-stage evolution model for submarine channel architecture on four styles of unstructured and structured slopes (Fig. 18). The model covers a range of spatial scales from the fundamental architectural unit (channel element) up to channel complex set.

6.3.1 Unstructured Slopes

Stage 1 – *Channel element formation and incision*. Through time, flows with sufficient energy develop a degree of confinement as flow vectors focus causing incision. A channel conduit is formed (channel element scale) as constructional levees simultaneously develop.

Subsequent channel elements incise further into the slope. Bank erosion associated with repeated cycles of channel element migration with incision results in the formation of a composite erosional surface (red surface).

Preservation of early channel elements of this phase is low; the high erosion rate means deposits formed through migration are typically self-cannibalised. Figure 18 therefore represents one of many potential configurations for early channel elements.

Stage 2 – *Migration and lower fill*. At a certain time, incision stops, and migration is preserved. Bends transform through combined downstream translation and expansion and are recorded in cross-section in the form of horizontally-stacked channel element deposits. Lateral migration between consecutive elements continues to modify the composite bounding surface, widening the complex. Mechanisms driving migration include a system's longitudinal profile reaching grade (Pirmez et al., 2000; Hodgson et al., 2011), an increase in base-level change (McHargue et al. 2011; Sylvester et al. 2011, 2012), and a decrease in sediment supply versus accommodation (Kneller, 2003; McHargue et al., 2011).

Stage 3 – *Aggradation and abandonment*. In the latter stages of the complex's development, lateral migration between channel elements decreases relative to the rate of aggradation forming oblique- to vertically-stacked channel elements deposits. Modifications to the composite bounding surface and the rate of change in channel complex width decreases. In planform, there is little change between consecutive elements with minor downstream translation recorded in obliquely-stacked channel element deposits.

The development of a stable planform and the subsequent aggradation of channel elements has been linked with waning flow energies relating to allogenic and autogenic controls (Peakall et al., 2000; Kolla et al, 2007; Jobe et al., 2016). The low density contrast between turbidity currents and the ambient fluid increases flow thickness and the potential for overspill and flow stripping, which promote overbank deposition and levee growth (Piper and Normark, 1983;

Imran et al., 1999; Peakall et al., 2000; Straub et al., 2008; Jobe et al., 2016). As flows wane and reduce in energy deposition increases which, promoted by the feedback between levee growth and channel thalweg aggradation, increases vertical aggradation and reduces the rate of change in channel complex width (Peakall et al., 2000). The development of external levees may also limit the ability of channel elements to migrate laterally, further increasing aggradation relative to migration (Peakall et al., 2000; Shumaker et al., 2018).

The end of turbidite sedimentation results in a waning flow and ultimately complex abandonment. Deposits begin to fill the final channel element erosional relief and subsequently the confining depositional relief created by external levee deposits.

Stage 4 – *Complex set development*. Reincision by a later complex (blue lines). Turbidite sedimentation resumes and channel elements successively reincise into the underlying channel complex. The second complex evolves in a way analogous to the first.

The degree of depositional relief remaining from the lower complex is a principal control on the degree of conformity between channel elements of the two complexes (McHargue et al., 2011). The model in figure 18 shows where a low degree of abandonment relief remains with only a depression between the external levees at the point of the initiation of the second channel complex. Consequently, there is little conformity in the stacking of channel elements of the two complexes.

6.3.2 Structured Slopes: Pre-channel Bathymetry

Stage 1 – *Channel element formation and incision*. A channel element forms in a way analogous to that described above, however, flows encounter pre-existing structural relief, which in this example is two thrust folds.

The first channel element diverts in the direction of the fold’s plunge passing around the pre-existing relief before continuing along its original course down regional slope. Successive channel elements form high-amplitude bends where structure has modified the local downslope direction, generating long wavelength bends in the course of the composite body (the early-stage complex) at a high angle to the regional slope. In section, repeated cycles of channel element migration and incision, analogous to that seen on an unstructured slope, generate a composite erosional surface, in this case with a stepped margin. Due to the high erosion rate associated with this phase deposits are largely self-cannibalised. The mechanism driving the cessation of incision is the same as for unstructured slope sections (see above).

Stage 2 – *Migration and lower fill*. Incision stops and migration is preserved in the stratigraphic record through horizontally-stacked channel element deposits. In planform, channel element bends, formed where structure has modified the local downslope direction, continue to expand progressively increasing sinuosity. Elsewhere on the diverted channel length migration may occur through downstream translation. Complex width increases as migration continues to modify the bounding surface.

Stage 3 – *Aggradation and abandonment*. Channel element migration decreases relative to the rate of aggradation. In planform, little change occurs between successive channel elements with deposits primarily stacking vertically, maintaining the previous channel element morphology. Modifications to the composite bounding surface and the rate of change in channel complex width decreases significantly. Turbidite sedimentation begins to wane as the complex is abandoned and filled.

Stage 4 – *Complex set development*. Incision of a later complex. The example in figure 18 illustrates a potential configuration when the folds remains inactive and abandonment relief of the past complex is low due to filling sediments. As a result, there is little conformity in the stacking of channel elements of the respective complexes, but the later complex is still confined by the external levees of the earlier system.

Channel entrenchment, like the incision of a second complex, and channel element sinuosity are primary processes associated with terrace development (Hansen et al., 2017).

Figure 18 illustrates the formation of a terrace through entrenchment, a configuration observed in channel one.

6.3.3 Structured Slopes: Coeval Positive Structural Bathymetry

Stage 1 – *Channel element formation and incision*. A channel element forms. Cycles of migration and incision begin forming a composite erosional surface, however, early in the process a thrust fold starts developing relief.

The development of relief continually modifies local slope gradient and leads to the preferential migration of bends toward the tip of the growing fold (or the direction of plunge), increasing the rate of migration relative to vertical incision. Consequently, the composite surface predominantly widens instead of deepening as successive channel elements stack away from the location of maximum shortening, toward the fold tip. The dominance of migration in a single direction during incision leads to preservation in this early phase.

Stage 2 – *Migration and lower fill*. A high-amplitude bend forms just up dip of the fold crest with channel elements continually expanding toward the fold tip substantially increasing channel element sinuosity and generating wide, highly asymmetric complex margins. Horizontally-stacked channel element deposits record the migration and bend development associated with this phase.

Stage 3 – *Continued migration and abandonment*. In contrast to unstructured slopes and pre-channel structured slopes, migration, bend growth and changes in complex width continue into the latter stages of complex development. As the fold continues to grow in relief, the associated lateral tilt causes channel elements to progressively shift toward the hangingwall syncline, substantially increasing the amplitude of the deflected bend. In section, channel elements continue to stack laterally with little to no aggradation between deposits. Migration continues until complex abandonment.

Stage 4 – *Complex set development*. Figure 18 illustrates a potential configuration where the fold remains active while the system is abandoned, partially folding the deposits of the earlier complex.

Typically, the abandonment relief of the most recently active complex is the primary control on the configuration of a later complex, however, on structurally active slopes, relief developed through deformation adds further complexity. In order for the system to develop to channel complex set scale and not avulse, confinement by the abandonment relief of the last system must exceed the change in relief due to structural growth. The example shown in figure 18 shows a disorganised stacking of channel elements of the two complexes with elements of the later complex (blue) cutting across the past channel element bends. The lack of conformity reflects the low abandonment relief of the earlier complex at the latter's initiation.

6.3.4 Structured Slopes: Coeval Negative Structural Bathymetry

Stage 1 – *Channel element formation and incision*. A channel element forms. Cycles of migration and incision begin forming a composite erosional surface occur concurrently with extensional faulting that develops negative relief.

Structure continually modifies local slope gradient and may initiate preferential migration toward the tip of the fault (or the direction of dip). Negative bathymetry associated with the hangingwall of the fault leads to reduced incision in this location.

Stage 2 – *Migration and lower fill*. High-amplitude bends form in the hangingwall of the extensional fault with channel elements continually expanding toward the fault tip, increasing channel element sinuosity. Horizontally-stacked channel element deposits record the migration and bend development associated with this phase.

Stage 3 – *Continued migration and aggradation prior to abandonment*. In contrast to unstructured slopes and pre-channel structured slopes, migration, bend growth and changes in complex width continue into the latter stages of complex development. The rate of aggradation increases as flow energy begins to wane (see section 6.3.1). Coeval aggradation and migration lead to the formation of thick obliquely-stacked channel element deposits. Migration and aggradation continue with bathymetry development until abandonment.

Stage 4 *– Complex set development*. Figure 18 illustrates a potential configuration where an extensional remains active while the system is abandoned.

Typically, the abandonment relief of the most recently active complex is the primary control on the configuration of a later complex, however, on structurally active slopes, relief developed through deformation adds further complexity. In order for the system to develop to channel complex set scale and not avulse, confinement by the abandonment relief of the last system must exceed the change in relief due to structural growth. The example shown in figure 18 shows an organised stacking of channel elements from the two complexes with elements of the later complex (blue) conforming to the morphology of past channel element bends (grey). Conformity of channel element stacking reflects a moderate-high abandonment relief at the point of latter channel complex's initiation.

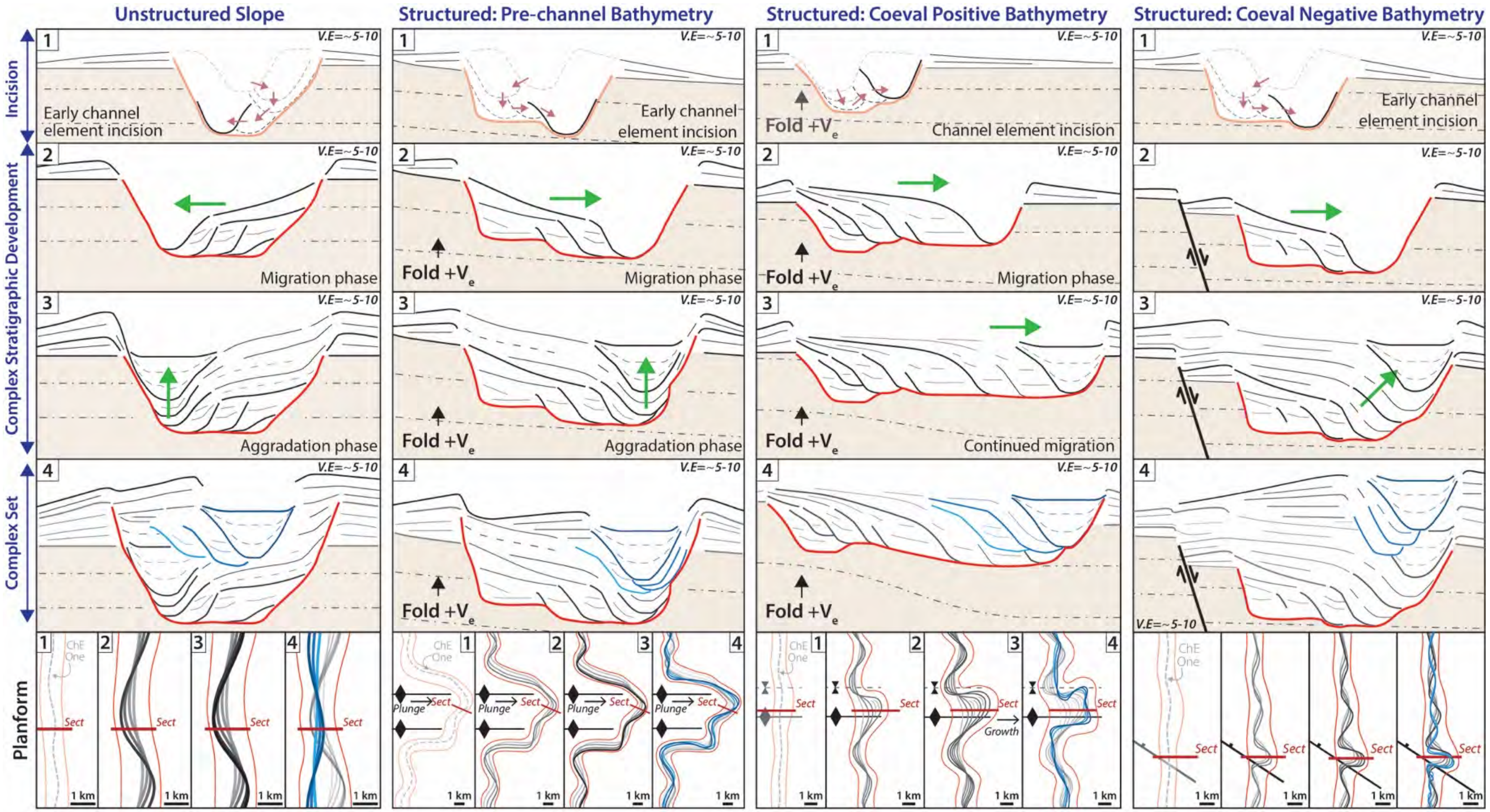

Figure 18. Conceptual model for the architectural evolution of submarine channels on four different styles of slope: unstructured, structured: pre-channel bathymetry, structured: coeval positive bathymetry, and structured: coeval negative bathymetry (Stages 1-3) Illustrate the development of a submarine channel complex. (Stage 4) Reincision of channel elements of a younger, second channel complex (blue) forming a channel complex set.

7. CONCLUSIONS

1. This study examines the architecture of two Pleistocene submarine channel systems as they interact with a range of gravity-driven structural styles on the southern Niger Delta slope. The systems extend for over 120 km and cross an undeformed translational domain, a strike-slip transfer zone, and two fold-and-thrust belts enabling the response of submarine channels to a variable structural template to be evaluated.
2. Depositional architectures, across a range of spatial scales from the fundamental architectural unit (a channel element) up to channel complex set scale, record the morphological response of the channel systems to tectonically driven changes in slope. Our results indicate submarine channel architecture is unambiguously linked to the underlying tectonic template with three clear end-member styles of channel-structure interaction classified as: pre-channel structural bathymetry, coeval positive relief, and coeval negative relief.
3. Across the unstructured slope of the translational domain, submarine channels display simple cross-sectional architectures with migration and subsequent aggradation well-represented, each by a distinct phase. Horizontally-stacked channel elements fill the lower erosional component of the complex and transition into an oblique to vertical stacking pattern in the later stages of complex development. This repeated arrangement of migration dominating the early stratigraphy, recording bend development through combined translation and expansion, and aggradation dominating the latter, indicates a decrease in the rate of growth in complex width and the rate of change in sinuosity relative to aggradation.
4. Where structural relief pre-dates channel inception, the principal adjustment to the system is in the initial channel course with early channel elements being forced around positive relief of the structure, generating long-wavelength bends in the complex's

course. This diversion, typically at a high angle to regional slope, allows migration and aggradation cycles analogous to those on an unstructured complex, with sinuosity development and growth in complex width occurring at an early stage.

5. Where structure is actively modifying the slope by creating positive relief, a channel complex will respond up-dip of the structure, by increasing the rate of migration relative to aggradation. Complexes form thin, wide cross-sectional architectures with aggradation between successive channel elements being significantly subdued or absent from the stratigraphic record altogether. Sinuosity and complex width continue to develop until the system is abandoned.
6. We use the stratigraphic architectures across the two channel systems to present four-stage models of submarine channel evolution under three different tectonic conditions: unstructured, pre-channel structural bathymetry, and coeval structural bathymetry (Fig. 18).
7. The results of this study illustrate the sensitivity of submarine channels to spatial and temporal variations in structural growth rate across fold-and-thrust belts. In order to further develop these concepts, future work quantifying channel element width, thickness, sinuosity, in addition to complex width, thickness, erosion:construction ratio is essential.

8. ACKNOWLEDGEMENTS

WHM is funded by the Natural Environment Research Council (NERC) Centre for Doctoral Training (CDT) in Oil & Gas. Data for the project were provided by PGS and the Nigerian Petroleum Directorate and we thank E. Taylor for facilitating access to data. We acknowledge a university software grant from Landmark-Halliburton and Paleoscan-Ellis. We thank anonymous reviewer and Rebecca Englert for their constructive comments on the manuscript. The data that support the findings of this study are available on request from the corresponding author.

8. REFERENCES

Abreu, V., Sullivan, M., Pirmez, C. and Mohrig, D., 2003, Lateral accretion packages (LAPs): an important reservoir element in deep water sinuous channels: Marine and Petroleum Geology, v. 20, no. 6–8, p. 631–648.

Benesh, N., Plesch, A., and Shaw, J.H., 2014, Geometry, kinematics, and displacement characteristics of tear-fault systems. An example from the deep-water Niger Delta: AAPG Bulletin, v. 98, no. 3, p. 465-482.

Bilotti, F. and Shaw, J.H., 2005, Deep-water Niger Delta fold and thrust belt modeled as a critical-taper wedge: The influence of elevated basal fluid pressure on structural styles: AAPG Bulletin, v. 89, no.11, p.1475-1491.

Broucke, O., Temple, F., Rouby, D., Robin, C., Calassou, S., Nalpas, T., and Guillocheau, F., 2004, The role of deformation processes on the geometry of mud-dominated turbiditic systems, Oligocene and Lower–Middle Miocene of the Lower Congo basin (West African Margin): Marine and Petroleum Geology, v 21, no. 3, p. 327-348.

Clark, I.R. and Cartwright, J.A., 2009, Interactions between submarine channel systems and deformation in deepwater fold belts: Examples from the Levant Basin, Eastern Mediterranean sea: Marine and Petroleum Geology, v. 26, no. 8, p. 1465-1482.

Clark, I.R. and Cartwright, J.A., 2011, Interactions between coeval sedimentation and deformation from the Niger Delta deepwater fold belt: SEPM special publication, v. 99, p.243-267.

Covault, J. A., Fildani, A., Romans, B. W., and McHargue, T., 2011, The natural range of submarine canyon-and-channel longitudinal profiles: Geosphere, v. 7, no. 2, p. 313-332.

Covault, J.A., Sylvester, Z., Hubbard, S.M., Jobe, Z.R., and Sech, R.P., 2016, The stratigraphic record of submarine-channel evolution: The Sedimentary Record, v. 14, p. 4-11.

Covault, J.A., Sylvester, Z., Hudec, M.R., Ceyhan, C., and Dunlap, D., 2019, Submarine channels 'swept' downstream after bend cutoff in salt basins: The Depositional Record, v. 6, p. 259-272.

Corredor, F., Shaw, J.H. and Bilotti, F., 2005, Structural styles in the deepwater fold and thrust belts of the Niger Delta: AAPG Bulletin, v. 89, no. 6, p.753-780.

Damuth, J., 1994, Neogene gravity tectonics and depositional processes on the deep Niger Delta continental margin: Marine and Petroleum Geology, v. 11, no. 3, p.320-346.

Deptuck, M.E., Steffens, G.S., Barton, M. and Pirmez, C., 2003, Architecture and evolution of upper fan channel-belts on the Niger Delta slope and in the Arabian Sea: Marine and Petroleum Geology, v. 20, no. 6–8, p. 649–676.

Deptuck, M.E., Sylvester, Z., Pirmez, C. and O'Byrne, C., 2007, Migration–aggradation history and 3-D seismic geomorphology of submarine channels in the Pleistocene Benin-major Canyon, western Niger Delta slope. Marine and Petroleum Geology, v. 24, no. 6–9, p. 406–433.

Deptuck, M. E., Sylvester, Z., & O'Byrne, C., 2012, Pleistocene seascape evolution above a "simple" stepped slope–Western Niger Delta. In B.E. Prather, M.E. Deptuck, D. Mohrig, B. Van Hoorn, & R.B. Wynn, Application of the principles of seismic geomorphology to continental-slope and base-of-slope systems: Case studies from seafloor and near-seafloor analogues. v. 99, p. 199–222: SEPM Society for Sedimentary Geology. 10.2110/pec.12.99.

Deptuck, M.E., and Sylvester, Z., 2018, Submarine Fans and Their Channels, Levees, and Lobes. In: Micallef, A., S. Krastel, and A. Savini, Submarine geomorphology. Submarine Geomorphology. Springer, London.

Doust, H., & Omatsola, E., 1989, Niger Delta. In J.D. Edwards, & P.A. Santogrossi Divergent/Passive Margin Basins, AAPG Memoir, (Eds.) (Vol. 48, pp. 201–238). Tulsa, USA: American Association of Petroleum Geologists.

Gardner, M.H., Borer, J.M., 2000. Submarine channel architecture along a slope to basin profile, Brushy Canyon Formation, West Texas. In: Bouma, A.H., Stone, C.G. (Eds.), Fine-grained Turbidite Systems. AAPG Memoir 72/SEPM Special Publication, v. 68. p. 195–214.

Gardner, M.H., Borer, J.M., Melik, J.J., Mavilla, N., Dechesne, M., Wagerle, R.D., 2003. Stratigraphic process-response model for submarine channels and related features from studies of Permian Brushy Canyon outcrops, West Texas: Marine and Petroleum Geology, v. 20, p. 757–788.

Hansen, L., Janocko, M., Kane, I., and Kneller, B., 2017, Submarine channel evolution, terrace development, and preservation of intra-channel thin-bedded turbidites: Mahin and Avon channels, offshore Nigeria: Marine Geology, v. 383, p. 146-167.

Heiniö, P. & Davies, R.J., 2006, Knickpoint migration in submarine channels in response to Fold Growth, Western Niger Delta: Marine and Petroleum Geology, v. 24, p. 434–449.

Hodgson, D.M, Di Celma, C.N., Brunt, R.L., and Flint, S.S., 2011, Submarine slope degradation and aggradation and the stratigraphic evolution of channel–levee systems: Journal of the Geological Society, v. 168, no. 3, p. 625-628.

Janocko, M., Nemec, W., Henriksen, S. and Warchoł, M., 2013, The diversity of deep-water sinuous channel belts and slope valley-fill complexes: Marine and Petroleum Geology, v. 41, p. 7–34.

Jobe, Z.R., Sylvester, Z., Parker, A.O., Howes, N.C., Slowey, N., and Pirmez, C., 2015, Rapid Adjustment of Submarine Channel Architecture To Changes In Sediment Supply: Journal of Sedimentary Research, v. 85, no. 6, p. 729-753.

Jobe, Z.R., Howes, N.C. and Auchter, N.C., 2016, Comparing submarine and fluvial channel kinematics: Implications for stratigraphic architecture: Geology, v. 44, no. 11, p. 931–934.

Jolly, B.A., Whittaker, A.C., and Lonergan, L., 2017, Quantifying the geomorphic response of modern submarine channels to actively growing folds and thrusts, deep-water Niger Delta: Geological Society of America Bulletin, v. 120, no. 9, p. 1123–1139.

Kane et al., 2010 (Kane, I. A., Catterall, V., McCaffrey, W. D. and Martinsen, O. J., 2010. Submarine channel response to intrabasinal tectonics: The influence of lateral tilt: AAPG Bulletin, v. 94, no. 2, p. 189-219.

Kneller, B., 2003, The influence of flow parameters on turbidite slope channel architecture: Marine and Petroleum Geology, v. 20, p. 901–910.

Kolla, V., Posamentier, H.W., and Wood, L.J., 2007, Deep-water and fluvial sinuous channels—Characteristics, similarities and dissimilarities, and modes of formation: Marine and Petroleum Geology, v. 24, no. 6-9, p. 388-405.

Krueger, S.W. and Grant, N.T., 2011, The growth history of toe thrusts of the Niger Delta and the role of pore pressure. In: K. McClay, J.H. Shaw, and J. Suppe, eds., Thrust fault-related folding: AAPG Memoir 94, p. 357–390.

Kulke, H., 1995, Nigeria. In: Kulke, H., ed., Regional Petroleum Geology of the World. Part II: Africa, America, Australia and Antarctica: Berlin, Gebrüder Borntraeger, p. 143-172.

Labourdette, R., and Bez, M., 2010, Element migration in turbidite systems: Random or systematic depositional processes? AAPG Bulletin, v. 94, no. 3, p. 345-368.

Mayall, M. and Stewart, I., 2000, The architecture of turbidite slope channels, GCSEPM Foundation 20th Annual Research Conference Deep-Water Reservoirs of the World, December 3-6, 2000, p. 578-586.

Mayall, M., Jones, E., and Casey, M., 2006, Turbidite channel reservoirs—Key elements in facies prediction and effective development: Marine and Petroleum Geology, v. 23, no. 8, p. 821-841.

Mayall, M., Lonergan, L., Bowman, A., James, S., Mills, K., Primmer, T., Pope, D., Rogers, L., and Skeene, R., 2010, The response of turbidite slope channels to growth-induced seabed topography: AAPG Bulletin, v. 94, no. 7, p. 1011-1030.

McArdle, N., and Ackers, M., 2012, Understanding seismic thin-bed responses using frequency decomposition and RGB blending: First Break, v. 30, no. 1956.

McHargue, T., Pyrcz, M.J., Sullivan, M.D., Clark, J.D, Fildani, A., Romans, B.W., Covault, J.A., Levy, M., Posamentier H.W., and Drinkwater, N.J., 2011, Architecture of turbidite channel systems on the continental slope: Patterns and predictions: Marine and Petroleum Geology, v. 28, no. 3, p. 728-743.

Mitchell, W. H., Whittaker, A., Mayall, M., Lonergan, L., and Pizzi, M., 2021, Quantifying the relationship between structural deformation and the morphology of submarine channels on the Niger Delta continental slope, Basin Research (*in press*)

Morgan, R., 2003, Prospectivity in ultradeep water: the case for petroleum generation and migration within the outer parts of the Niger Delta apron: Geological Society, London, Special Publications, v. 207, no. 1, p. 151-164.

Paull, C.K., Talling, P.J., Maier, K.L. et al., 2018, Powerful turbidity currents driven by dense basal layers: Nature Communications, v. 9, 4114. 10.1038/s41467-018-06254-6

Peakall, J., McCaffrey, W.D., Kneller, B.C., 2000, A process model for the evolution, morphology, and architecture of sinuous submarine channels: Journal of Sedimentary Research, v. 70, p. 434–448.

Pizzi, M., Lonergan, L., Whittaker, A.C., Mayall, M., 2020, Growth of a thrust fault array in space and time: An example from the deep-water Niger delta: Journal of Structural Geology. 10.1016/j.jsg.2020.104088

Pirmez, C., R.T. Beaubouef, S.J. Friedmann, & D.C. Mohrig, 2000, Equilibrium profile and baselevel in submarine channels: examples from late pleistocene systems and implications for architecture in deepwater reservoirs. In: Deep-Water Reservoirs of the World (Eds.), 20th Annual GCS-SEPM Foundation Bob F. Perkins Research Conference, p. 782–805. SEPM.

Posamentier, H.W., Kolla, V., 2003, Seismic geomorphology and stratigraphy of depositional elements in deep-water settings: Journal of Sedimentary Research, v. 73, p. 367–388.

Rouby, D., Nalpas, T., Jermannaud, P., Robin, C., Guillocheau, F., and Raillard, S., 2011, Gravity driven deformation controlled by the migration of the delta front: The Plio-Pleistocene of the Eastern Niger Delta: Tectonophysics, v. 513, no. 1-4, p. 54-67.

Shumaker, L., Z. Jobe, S. Johnstone, L. Pettinga, D. Cai., & J. Moody, 2018, Controls on submarine channel-modifying processes identified through morphometric scaling relationships: Geosphere, v.14, no.5, p. 2171-2187.

Sprague, A.R.G., Sullivan, M.D., Campion, K.M., Jensen, G.N., Goulding, F.J., Garfield, T.R., Sickafoose, D.K., Rossen, C., Jennette, D.C., Beaubouef, R.T., Abreu, V., Ardill, J., Porter, M.L., Zelt, F.B., 2002. The physical stratigraphy of deep-water strata: a hierarchical approach to the analysis of genetically related stratigraphic elements for improved reservoir prediction (abstract). In: American Association of Petroleum Geologists, Annual Meeting, March 10–13, 2002, Houston, Texas, Official Programpp. A167.

Sprague, A.R.G., Garfield, T.R., Goulding, F.J., Beaubouef, R.T., Sullivan, M.D., Rossen, C., Cmapion, K.M., Sickafoose, D.K., Abreu, V., Schellpeper, M.E., Jensen, G.N., Jennette, D.C., Pirmez, C., Dixon, B.T., Ying, D., Ardill, J., Mohrig, D., Porter, M.L., Farrell, M.E., Mellere, D., 2005, Integrated slope channel depositional models: The key to successful prediction of reservoir presence and quality in offshore West Africa. In: CIPM, Cuarto E-Exitep 2005, February 20–23, 2005, Veracruz, Mexicopp. 1–13.

Sylvester, Z., Pirmez, C. and Cantelli, A., 2011, A model of submarine channel-levee evolution based on channel trajectories: Implications for stratigraphic architecture: Marine and Petroleum Geology, v. 28, no. 3, 716–727.

Sylvester, Z. and Covault, J.A., 2016, Development of cutoff-related knickpoints during early evolution of submarine channels: Geology, v. 44, no. 10, p. 835–838.

Totake, Y., Butler, R., Bond, C., & Aziz, A., 2018, Analyzing structural variations along strike in a deep-water thrust belt: Journal Of Structural Geology, v.108, p.213-229. doi: 10.1016/j.jsg.2017.06.007

Wu, J.E., McClay, K., Frankowicz, E., 2015. Niger Delta gravity-driven deformation above the relict Chain and Charcot oceanic fracture zones, Gulf of Guinea: Insights from analogue models: Marine and Petroleum Geology, v. 65, p. 43–62.

Wynn, R.B., Cronin, B.T. and Peakall, J., 2007, Sinuous deep-water channels: Genesis, geometry and architecture: Marine and Petroleum Geology, v. 24, no. 6, p.341-387.

Wynn, R. B., Talling, P. J., Masson, D. G., Le Bas, T. P., Cronin, B. T., Stevenson, C. J, 2012, The Influence of Subtle Gradient Changes on Deep-Water Gravity Flows: A Case Study From the Moroccan Turbidite System. In: Prather, B. E., Deptuck, M. E., Mohrig, D., Van Hoorn, Wynn, R. B., Talling, P. J., Masson, D. G., Le Bas, T. P., Cronin, B. T., & Stevenson, C. J., 2012, The influence of subtle gradient changes on deep-water gravity flows: A case study from the moroccan turbidite system. In B. E. Prather, M. E. Deptuck, D. Mohrig, B. Van Hoorn, & R. B. Wynn (Eds.) Application of the principles of seis- mic geomorphology to continental-slope and base-of-slope systems: Case studies from seafloor and near-seafloor analogues. v. 99, p. 371–383. SEPM Special Publication, SEPM.